

## CONTENTS — M through Z

---

The Martian Relief's Dichotomy and Planetary Axial Structural Symmetry <i>G. F. Makarenko</i> .....	4008
Crustal Evolution of the Protonilus Mensae Area, Mars <i>G. E. McGill, S. E. Smrekar, A. M. Dimitriou, and C. A. Raymond</i> .....	4003
Loading-induced Stresses and Topography Near the Martian Hemispheric Dichotomy Boundary <i>P. J. McGovern and T. R. Watters</i> .....	4034
Topographic Change of the Dichotomy Boundary Suggested by Crustal Inversion <i>G. A. Neumann</i> .....	4033
Tectonic Consequences of Dichotomy Modification by Lower Crustal Flow and Erosion <i>F. Nimmo</i> .....	4006
Glacial Modification of the Martian Crust in Aeolis Region, Mars <i>J. Nussbaumer</i> .....	4018
Degree-1 Mantle Convection as a Process for Generating the Martian Hemispheric Dichotomy <i>J. H. Roberts and S. Zhong</i> .....	4028
Control of Exposed and Buried Impact Craters and Related Fracture Systems on Hydrogeology, Ground Subsidence/Collapse, and Chaotic Terrain Formation, Mars <i>J. A. P. Rodriguez, S. Sasaki, J. M. Dohm, K. L. Tanaka, H. Miyamoto, V. Baker, J. A. Skinner Jr., G. Komatsu, A. G. Fairén, and J. C. Ferris</i> .....	4015
Outflow Channel Sources, Reactivation and Chaos Formation, Xanthe Terra, Mars <i>J. A. P. Rodriguez, S. Sasaki, J. M. Dohm, K. L. Tanaka, H. Miyamoto, V. Baker, J. A. Skinner Jr., G. Komatsu, A. G. Fairén, and J. C. Ferris</i> .....	4016
Mass-Wasting of the Circum-Utopia Highland/Lowland Boundary: Processes and Controls <i>J. A. Skinner Jr., K. L. Tanaka, T. M. Hare, J. Kargel, G. Neukum, S. C. Werner, and J. A. P. Rodriguez</i> .....	4031
Subsurface Structure of the Ismenius Area and Implications for Evolution of the Martian Dichotomy and Magnetic Field <i>S. E. Smrekar, C. A. Raymond, and G. E. McGill</i> .....	4021
Endogenic Mechanisms for the Formation of the Martian Crustal Dichotomy: Hypotheses and Constraints <i>S. C. Solomon</i> .....	4024
Triggering the End of Plate Tectonics by Forced Climate Changes <i>M. G. Spagnuolo and J. Dohm</i> .....	4001
Mars Impact Energy Analysis in Support of the Origin of the Crustal Dichotomy and Other Anomalies <i>G. R. Spexarth</i> .....	4002

Topographic and Geomorphic Modification History of the Highland/Lowland Dichotomy Boundary of Mars: I. Noachian Period <i>K. L. Tanaka</i> .....	4023
Topographic and Geomorphic Modification History of the Highland/Lowland Dichotomy Boundary of Mars: II. Hesperian and Amazonian Periods <i>K. L. Tanaka</i> .....	4030
Long Wavelength Topography of the Dichotomy Boundary in Northern Terra Cimmeria: Evidence for Flexure of the Southern Highlands <i>T. R. Watters, P. J. McGovern, and R. P. Irwin III</i> .....	4032
Effect of the Dichotomy on Mantle Plume Locations <i>M. J. Wenzel, M. Manga, and A. M. Jellinek</i> .....	4035
On the Dynamic Origin of the Crustal Dichotomy and Its Implications for Early Mars Evolution <i>S. J. Zhong, J. H. Roberts, and A. McNamara</i> .....	4019

## THE MARTIAN RELIEF'S DICHOTOMY AND PLANETARY AXIAL STRUCTURAL SYMMETRY.

**Makarenko G. F.**, General Physics Institute of RAS, 119991 Moscow, Vavilov str. 38

[mkrn@kapella.gpi.ru](mailto:mkrn@kapella.gpi.ru)

[www.gpi.ru/~mkrn/lpsr](http://www.gpi.ru/~mkrn/lpsr)

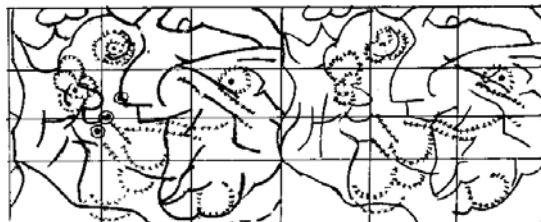
**The basic property of the Earth is axial structural symmetry of its outer shell** [1,2]. This indisputable phenomenon is not visible from the space (oceans). Rejecting the displacement of earthen shell (plate drifting) **only** allows to compare Earthen tectonic tracteries with the seams on other planets. Similarity of large dislocated zones position on the Earth and Mars are reflected in relief, in faults picture and in Earthen structures without relief.

Confront the 60 martian meridian with the 0 Earthen meridian [3]. We see (upper Fig., Earth – lines, Mars – points, dotted lines and small rings - martian volcanoes) the coincidence of huge arcs on the planets in their south hemispheres, arcs bend near 0 and 180 meridians of the Earth. Here we have ocean ridges curves. The form of the south arc on the Mars is accented by the margin of Argir depression and on the other globe side – by Eridania stair, eastwards of crater Kepler. Alike near latitude planet fault systems are placed around the equator. On the Mars their images are fault seams (Mariner canyon; on another planet side – Amentes set-off and Eolyda rise). They have branches to NE also around 60 and 260-240 meridians accordingly.

Olimp is a huge martian volcano, with ambient rings with lavas. Let us “relax” the volcanic “disk” (altitude to basis ratio 1 : 20), i.e. embed it to the martian entrails. Their images on the Earth are the rears of hercinides of Apalachians and Uoashito with their coats of ocean and Mexican Bay's lavas. On the other Earthen side there are basalt lavas of Eymeshan Plato at the Sikkan-Yunnan fold zone rear. Southwards we see young lavas among the young island arcs. Patera Alba is an appreciable volcanic place. Its reflection on the Earth are basalts of Atlantic arc Corner-Miln and lavas in the Japan Isles rear.

On the scheme (Fig. below) from Martian

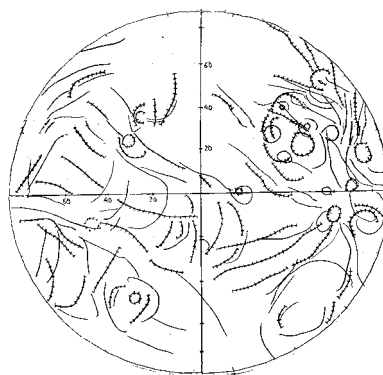
map [4] the structural lines and volcanoes of “Olimp's” side (lines with trites) and of the other side (lines) are shown.



0-Earth (60W Mars)

Six volcanoes- now rings only- fix the Olimp's place on this planet side: near the center Flammarion, Antoniadi (N 25 ), Schroeter (0 ), Tichonravov (N 13 ), Cassini (N 24 ), Quenisset (N 35 ) and Rudaux (N 38 ).

This volcanic field looks alike trapp Earthen field with long living deep channels.



The Earth and the Mars are twins (both without the “plate tectonics” and without the grand impacts).

The relief's Martian dichotomy (N-S) is clear; the relief's Earthen dichotomy (W-N hemispheres) is evidential too.

**References:** [1] Makarenko G.F. (1998) Japan islands... Proc. Int. Simp. NCGT, Tsukuba, Japan, p.244-249 (Engl), [2] Makarenko G.F. (1997) Periodicity of basalts, biocrisises... Mosc. Geoinformmark, 95p. (Rus). [3] Merrill R. (1999) Science. Vol 284, 28 May 1495-1502. [4] Mars map 1:25 mln., Dresden Un. Of Techn. Ed. M. Buchroither, Cons. MIIGAIG., 2001.

**CRUSTAL EVOLUTION OF THE PROTONILUS MNSAE AREA, MARS.** G. E. McGill<sup>1</sup>, S.E. Smrekar<sup>2</sup>, A.M. Dimitriou<sup>1,3</sup>, and C.A. Raymond<sup>2</sup>, <sup>1</sup> Dept. of Geosciences, Univ. of Massachusetts, Amherst, MA (gmccgill@geo.umass.edu). <sup>2</sup> Jet Propulsion Lab., MS 183-501, 4800 Oak Grove Dr., Pasadena, CA, <sup>3</sup> SLR Alaska, 2525 Blueberry Rd., Suite 206, Anchorage, AK.

Despite research by numerous geologists and geophysicists, the age and origin of the martian crustal dichotomy remain uncertain. Models for the origin of this dichotomy involve single or multiple impact, mantle megaplumes, primordial crustal asymmetry, and plate tectonics [1 - 10]. Most of these models imply a Noachian age for the dichotomy. A major problem common to all genetic models is the difficulty separating the features resulting from the primary cause for the dichotomy from features due to younger faulting, impact cratering, volcanism, deposition, and erosion.

The boundary between northern lowlands and southern highlands (the dichotomy boundary) approximates a small circle that ranges in latitude from about  $-10^{\circ}$  in Elysium Planitia to about  $+45^{\circ}$  north of Arabia Terra. For much of its length the boundary is characterized by relatively steep scarps separating highland plateau to the south from lowland plains to the north, generally with a complex transition zone on the lowland side of these scarps [11]. These scarps are almost certainly due to normal faulting. The type fretted terrain [12], which defines the boundary in north-central Arabia Terra, also is characterized by scarps but has undergone a more complex history of faulting and dissection [13]. In some places, notably in the Acidalia Planitia region, the dichotomy boundary is gradational. In the Tharsis region the boundary is obscured by younger volcanics.

The present study concerns the segment of dichotomy boundary between about  $50^{\circ}\text{E}$  and  $90^{\circ}\text{E}$  ( $310^{\circ}$ - $270^{\circ}\text{W}$ ), within the Ismenius Lacus and Cassius quadrangles. This site was chosen because: 1) within part of the site the boundary is a single well defined scarp  $\sim 2.5$  km high, 2) parallel to this scarp are several grabens, which support an extensional origin for the boundary scarp, and which also provide a means to estimate strain, 3) erosion appears not to be extreme, 4) the geology and structural history allow constraining the age of the boundary scarp, and 5) there are areal correlations among topography, geology, remanent magnetism, and gravity anomalies. The combination of tractable geology with magnetic and gravity data provides a rare opportunity to infer the evolution of the crust and mantle along the highland/lowland boundary.

Terrains within the study site may be divided into three structural blocks based on surface morphology and elevation. From southwest to northeast these are: 1) highland plateau, 2) lowland bench, and 3) lowland plains [14]. The highland plateau block is within the large region Arabia Terra, which is somewhat anomalous because it is topographically lower than most highland areas despite its highland crater population. The highland plateau has been resurfaced following accumulation of most of its large craters. The crater age of the highland plateau is Early Noachian; the age for craters younger than the resurfacing event is Middle Noachian. High resolution THEMIS and MOC images indicate that resurfacing was accomplished at least in part by deposition of a layer of material that is thin enough to permit the rims of older craters larger than a few km in diameter to show

through as inliers. Thus the post-resurfacing crater age is interpreted to be the age of the material deposited on the highland basement.

The boundary between the highland plateau and the lowland bench is a fault or zone of faults. The lowland bench is 2-3 km lower than the highland plateau, and is characterized by an abundance of knobby inliers projecting through a younger layer of smooth plains material. Some of these knobs clearly define circles that are inferred to be structurally disrupted crater rims ("knob ghosts"). A count of all craters and knob ghosts yields a Late Noachian age. However, the presence of the knob ghosts indicates that the basement surface under the lowland bench has experienced greater structural disruption than the basement of the highland plateau where rims of large, ancient craters, although degraded, have not been dissected into rings of knobs. The basement of the lowland bench also is partially covered by plains material that is similar to the material underlying the lowland plains block. Thus it is very likely that the age of the basement beneath the lowland bench is similar to the age of the basement beneath the highland plateau; that is, Early Noachian. This is consistent with the basement age determined for the entire lowland using all craters visible in images plus "Quasi-Circular Depressions" (QCD's) visible only in MOLA digital terrain models [15].

Is it possible that the scarp separating highland plateau from lowland bench is erosional rather than structural? The highland plateau and lowland bench have similar basement ages. It is not possible for the scarp to be older than these basement ages because it could not have survived formation of the craters yielding these basement ages. If the scarp formed by erosion after the cratering of the highland plateau and lowland bench basement, then on the order of the scarp height (2.5 km) of material must have been removed over what is now the lowland bench. This depth of erosion would have completely destroyed the rims of all of the craters used to date the lowland bench basement. It thus appears to be impossible to create the current topography within the Protonilus Mensae area by extensive erosion alone.

The boundary between the lowland bench and the lowland plains is characterized by the abrupt loss of the knobs that are so abundant on the lowland bench. This boundary is parallel to and about 400 km NE of the scarp that separates highland plateau and lowland bench. The loss of the knobby topography along this boundary is most likely due to an increase in thickness of smooth plains material, resulting in complete burial of the knobs in the lowland plains block. The abruptness of this loss of knobby topography suggests that the lowland bench/lowland plains boundary is a fault, down on the NE [14]. There is no topographic signature of this fault other than the loss of knobby topography, indicating that its fault scarp has been completely destroyed or buried. The minimum vertical displacement needed to completely bury the knobs of the lowland bench block is about one kilometer; the actual displacement is probably greater

but is not constrained. Poorly defined ridges that are similar to wrinkle ridges occur in the lowland plains block. These ridges are locally parallel to the dichotomy boundary. The age of the smooth surface material in the lowland plains block is Late Hesperian [11,14]. The smooth plains material surrounding the knobs on the lowland bench is continuous with the plains material in the lowland plains block, and thus also is inferred to be Late Hesperian.

Both the dichotomy boundary scarp separating highland plateau from lowland bench, and the buried fault separating lowland bench from lowland plains cut basement rocks of Early Noachian age. The boundary scarp also cuts the Middle Noachian resurfacing material of the highland plateau. Thus the old age limit for faulting in this area is Middle Noachian. The smooth plains material underlying the lowland plains is also present as a thin veneer on the lowland bench. This plains material embays the boundary scarp in places, and it buries the buried fault, indicating that the young age limit for faulting in this area is Late Hesperian. The relative age range Middle Noachian-Late Hesperian is interpreted to correspond to an age range in years of 3.9-3.1 Ga [16]. The old limit is only 140 Ma younger than the young age limit for lowland basement as determined using QCD's [17].

The dichotomy boundary scarp and the scarps bordering the grabens that are present SW of the boundary scarp have slopes in the range 13-21°; thus, as we would expect, these scarps are degraded from the presumed ~60° slope of a pristine normal fault scarp. Using MOLA altimetry profiles and assuming 60° fault dips, the extensional strain in the immediate vicinity of the dichotomy boundary scarp is determined to be ~3.5%

The lowland bench block is part of an extensive transitional zone between highland and lowland. Lowland bench crater ages determined in this study are completely consistent with crater ages determined for this entire transitional zone [11]. Furthermore, the old age limit on dichotomy boundary faulting in the Amenthes area [18] is similar to or perhaps slightly younger than the old limit in this study area. Thus the present morphology of the dichotomy boundary for segments characterized by scarps is due to faulting between Middle Noachian and Late Hesperian. The remanent magnetic field and gravity anomalies correlate with the morphology and structure of the dichotomy boundary zone in the Protonilus Mensae area, providing an excellent opportunity to model the crust and upper mantle where there are relatively robust geological constraints. The geology and topography of the study site are consistent with either the creation of the dichotomy by faulting between Middle Noachian and Late Hesperian, or with an earlier creation followed by crustal-scale processes that were responsible for the faulting. We currently are exploring the latter possibility.

- [1] Wilhelms, D.E., and S.W. Squyres (1984) *Nature*, 309, 138-140. [2] Frey, H., and R.A. Schultz (1988) *Geophys. Res. Lett.*, 15, 229-232. [3] Mutch, T.A., R.E. Arvidson, J.W. Head, III, K.L. Jones, and R.S. Saunders (1976) *The geology of Mars*, Princeton Univ. Press. [4] Wise, D.U., M.P. Golombek, and G.E. McGill (1979a) *Icarus*, 38, 456-472. [5] Wise, D.U., M.P. Golombek, and G.E. McGill (1979b) *J. Geophys. Res.*, 84, 7934-7939. [6] Breuer, D., D.A. Yuen, and T. Spohn (1997) *Earth Planet. Sci. Lett.* 148, 457-469. [7] Breuer, D., D.A. Yuen, T. Spohn, and S. Zhang (1998) *Geophys. Res. Lett.* 25, 229-232. [8] Zhong, S., E. and M.T. Zuber (2001) *Earth Planet. Sci. Lett.*, 189, 75-84. [9] Sleep, N.H. (1994) *J. Geophys. Res.*, 99, 5639-5655. [10] Lenardic, A., F. Nimmo, and L. Moresi (2004) *J. Geophys. Res.*, 109, doi: 10.1029/2003JE002172. [11] Frey, H., A.M. Semeniuk, J.A. Semeniuk, and S. Tokarcik (1988) *Proc. 18<sup>th</sup> Lunar Planet. Sci. Conf.*, 679-699. [12] Sharp, R.P. (1973) *J. Geophys. Res.*, 78, 4073-4083. [13] McGill, G.E. (2000) *J. Geophys. Res.* 105, 6945-6959. [14] Dimitriou, A.M. (1990) M.S. Thesis, Univ. Massachusetts, Amherst. [15] Frey, H.V., J.H. Roark, K.M. Shockey, E.L. Frey, and S.E.H. Sakimoto (2002) *Geophys. Res. Lett.*, 29, 10.1029/2001 GL013832. [16] Hartmann, W.K., and G. Neukum (2001) in Kallenback, R., J. Geiss, and W.K. Hartmann, eds., *Chronology and evolution of Mars*, Kluwer Academic Publishers, 165-194. [17] Frey, H.V. (2004) *Lunar Planet. Sci. XXXIV*, Abstract #1382. [18] Maxwell, T.A., and G.E. McGill (1988) *Proc. 18th Lunar Planet. Sci. Conf.*, 701-711

**Loading-induced Stresses and Topography Near the Martian Hemispheric Dichotomy Boundary.** P. J. McGovern<sup>1</sup> and T. R. Watters<sup>2</sup>, <sup>1</sup>Lunar and Planetary Institute, 3600 Bay Area Blvd., Houston TX 77058, ([mcgovern@lpi.usra.edu](mailto:mcgovern@lpi.usra.edu)), <sup>2</sup>Center for Earth and Planetary Studies, National Air and Space Museum, Smithsonian Institution, Washington D.C. 20560 ([twatters@nasm.si.edu](mailto:twatters@nasm.si.edu)).

**Introduction:** The dichotomy between the northern and southern hemispheres of Mars is one of the fundamental physiographic features of the planet. The dichotomy is manifested in the topography, geology, tectonics, cratering record, magnetic field, and crustal structure. The origin of the crustal dichotomy between northern (relatively thin, constant thickness) and southern (relatively thick and thickening southward) crustal provinces [1] appears to date to the earliest Noachian [2], a period with scant remaining traces in the geologic record. However, subsequent geologic and tectonic events may contain clues as to the nature of the hemispheric dichotomy.

The Eastern Hemisphere Dichotomy Boundary (or “EHDB”) of Mars between 40°E (western Arabia Terra) and 160°E (Terra Cimmeria) is characterized by a prominent topographic scarp (several km in height), compressional features on the highlands side and extensional features on the boundary ramp [3, 4]. Loading of the lithosphere due to emplacement of volcanic or sedimentary material on the lowlands side, erosion on the highlands side, and an episode of global compression in the Hesperian may be responsible for the observed topography and tectonics. A broken-plate flexural model with elastic lithosphere thickness  $T_e = 31\text{--}36$  km provided a good fit to Mars Orbiter Laser Altimeter (MOLA) topography data across the EHDB [3].

**Method:** We use the finite element code Tekton [5] to model the response of the Martian crust and mantle to surface loads emplaced near the hemispheric dichotomy boundary. The model grid accounts for crustal and mantle structure in the vicinity of EHDB, as constrained by studies of gravity and topography [e.g., 1, 6–8]. The grid exhibits plane strain geometry and extends 2720 km horizontally and 1720 km vertically. In the left-hand section of the model, a crust of 40 km thickness (representing the northern lowlands of Mars) lies at the surface. In the right-hand section (representing the southern uplands), the crust is ~55 km thick, yielding isostatic compensation for a 3 km difference in topography between “North” and “South” sections [e.g., 3] corresponding to densities  $\rho_{\text{crust}} = 2900 \text{ kg/m}^3$  and  $\rho_{\text{mantle}} = 3500 \text{ kg/m}^3$ . A section of elements 160 km wide, cosine tapered, accommodates the corresponding transition in crustal thickness. These dimensions simulate the change in elevation and width

of the dichotomy boundary in the Eastern Hemisphere of Mars.

The finite element grid starts in an isostatic configuration to reflect likely conditions at the time the crustal thickness variations were established. Rheological parameters are determined by flow laws for diabase [9] and olivine [10], as functions of temperature governed by pre-set thermal gradients. Models termed “uniform” assign material properties in horizontal rows of elements based on the thermal gradient the northern highlands. We also explore the effects of lateral variations in thermal gradients by assigning independent values to the lowlands, transition region, and highlands. Three types of loading were modeled. For depositional loading, density was increased in a line of elements “northward” (to the left) of the boundary ramp to represent the emplacement of sediments or volcanic material in the northern lowlands. Conversely, erosional loading southward of the dichotomy was modeled by decreasing element densities. An episode of large-scale compression (i.e., the event that caused widespread compressional ridged plains formation in the early Hesperian [e.g., 11, 12]) was modeled by moving the lateral boundaries of the model inward by an amount corresponding to 0.2% horizontal strain.

**Results:** Topographic profiles resulting from several types of dichotomy boundary loading are shown in Figure 1. Models with purely surface depositional loads in the northern lowlands do not generate appreciable flexural topography on the highlands side. For the thermal gradients (10 and 15 K/km) used here, lower crustal elements exhibit low viscosities that allow relaxation of surface topography [e.g., 13–16], such as flexurally induced arching [13]. The depositional loads induce horizontal extension in the highlands proximal to the boundary, consistent with the observed presence of normal faulting at the dichotomy boundary [e.g., 3], but the Mohr-Coulomb failure criterion is not exceeded. Erosional unloading of the highlands results in flexural uplift of the margin (Figure 1), but the plotted curve substantially overestimates the actual topography if the eroded material is removed from the surface. The curve in Figure 1 could represent the actual topography only for an erosive mechanism that removed subsurface material while leaving the surface relatively undisturbed, such as hydrothermal circulation or karst formation. Erosional unloading produces horizontal extension in the unloaded area,

and the failure criterion is satisfied over most of this area.

Models with large-scale compression yield predictions of ubiquitous thrust faulting at the surface of the model. The “uniform” models and models with higher thermal gradients in the lowlands than in the highlands produce more pervasive thrust faulting in the lowlands than in the highlands, a consequence of weaker lithosphere in the former. This finding is consistent with the presence of numerous ridges in the northern plains [11–12], although such ridges are not prevalent near the dichotomy boundary. In contrast, models with higher thermal gradients in the highlands than in the lowlands result in more pervasive thrusting in the highlands. This result is in accord with presence of compressional faults in the highlands near the EHDB [3, 4]. Intriguingly, large-scale compression can also produce a topographic arch on the highland side of the dichotomy boundary. For models with enhanced thermal gradients in the highlands, such relief resembles the observed topography (Figure 1). This feature is essentially a buckling instability, localized by the contrast in rheological structure at the dichotomy boundary.

How was the characteristic topographic profile of the EHDB derived? Our results suggest that simple depositional surface loading of continuous lithospheric plate is not a likely explanation [see 17]. An erosive mechanism that removes subsurface material while preserving topography can qualitatively reproduce an arched profile (Figure 1), but such a scenario is unlikely given the evidence for removal of surface deposits at the EHDB. Analytic flexure modeling suggests that broken lithospheric plates provide the best fits to EHDB topography [17], although it is unclear how the lithosphere beneath the boundary becomes discontinuous. The compression-induced scenario presented above for generating arched boundary relief relies on lateral lithospheric heterogeneity (rather than sharp discontinuities), generated by variations in thermal gradient. The most successful such model (Figure 1) invokes elevated thermal gradients in the highlands. Such gradients could result from a higher concentration of radiogenic heat-producing elements in the thicker southern highlands crust, or from a mantle upwelling beneath the highlands [18].

**Future Directions.** This reconnaissance of parameter space has only considered viscoelastic behavior in plane-strain geometry. Further modeling will include the effects of plastic yielding, in order to better constrain the interaction of the various loading processes and the spatial and temporal distributions of faulting. We will also use Tekton’s spherical axisymmetric geometry capabilities to explore the effects of planetary curvature.

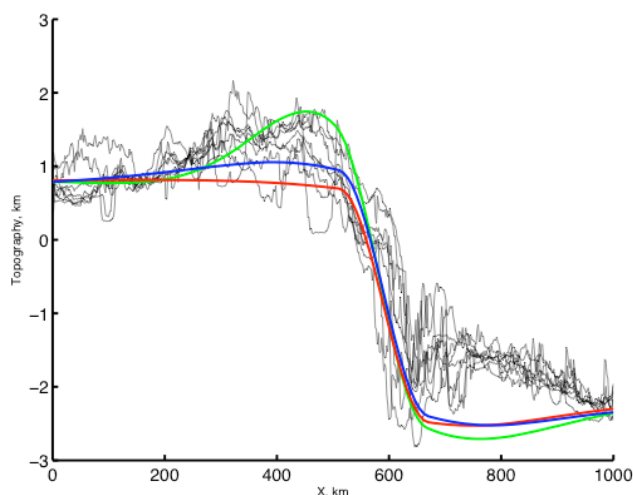


**Figure 1.** Topography of the Eastern Hemisphere Dichotomy Boundary (EHDB) for nine profiles (black lines, from [3]), and surface topography for three models of lithospheric loading and deformation. South is to the left. Red line: “uniform” model subject to surface depositional loading in the lowlands. Blue line: same as red line but after erosive unloading in the highlands. Green line: model with enhanced thermal gradient in the highlands, after 0.2% horizontal compressive strain.

**References:** [1] Zuber, M. T., et al. (2000) *Science*, 287, 1788. [2] Frey, H. (2002) *GRL*, 29, doi 10.1029/2001GL013882. [3] Watters, T. R. (2003) *Geology*, 31, 271. [4] Watters, T. R. (2003) *JGR*, 108, 8-1, 8-12. [5] Melosh, H. J., and Raefsky, A. (1983), *JGR*, 88, 515. [6] McGovern, P. J., et al. (2002) *JGR*, 107, doi 10.1029/2002JE001854. [7] McKenzie, D. (2002) *EPSL*, 195, 1. [8] Neumann, G. A., et al. (2004) *JGR*, 109, in press. [9] Caristan, Y. (1982), *JGR*, 87, 6781. [10] Karato, S.-I., et al. (1986), *JGR*, 91, 8151. [11] Withers, P., and Neumann, G. A. (2001) *Nature*, 410, 610. [12] Head, J. W., et al. (2002), *JGR*, 107, doi 10.1029/2000JE001445. [13] McGovern, P. J., and Watters, T. R. (2004), *LPS*, XXXV, abstract 2148. [14] Guest, A., and Smrekar, S. E. (2004), *LPS XXXV*, abstract 1362. [15] Nunes, D. C., et al. (2004), *JGR*, 109, doi10.1029/2003JE002119, 2004. [16] Nimmo, F. and Stevenson, D. J. (2001) *JGR*, 106, 5085. [17] Watters, T. R., et al. (2004), this volume. [18] Wüllner, U., and Harder, H. (1998), *PEPI*, 109, 129.



**TOPOGRAPHIC CHANGE OF THE DICHOTOMY BOUNDARY SUGGESTED BY CRUSTAL INVERSION.** G. A. Neumann<sup>1,2</sup>, <sup>1</sup> *Department of Earth, Atmospheric and Planetary Sciences, Massachusetts Institute of Technology, Building 54, 77 Massachusetts Avenue, Cambridge, MA 02139-4307, (neumann@tharsis.gsfc.nasa.gov),* <sup>2</sup> *Laboratory for Terrestrial Physics, Code 926, NASA/Goddard Space Flight Center, Greenbelt, MD 20771.*

Linear negative gravity anomalies in Acidalia Planitia along the eastern edge of Tempe Terra and along the northern edge of Arabia Terra have been noted in Mars Global Surveyor gravity fields [1, 2, 3]. Once proposed to represent buried fluvial channels [4, 5], it is now believed that these gravity troughs mainly arise from partial compensation of the hemispheric dichotomy topographic scarp [6]. A recent inversion for crustal structure [7] finds that mantle compensation of the scarp is offset from the present-day topographic expression of the dichotomy boundary. The offset suggests that erosion or other forms of mass wasting occurred after lithosphere thickened and no longer accommodated topographic change through viscous relaxation.

**Introduction** Using MOLA topography and the most recent gravity field from MGS and Mars Odyssey tracking, jgm95h01, we invert for the crustal structure required to plausibly match gravity, crustal topography and density variations to degree and order 90, allowing for the effects of power-law constraints applied at degrees 60 and higher to reduce noise primarily in the gravity solution. The effective resolution (minimum resolved pixel size) of this inversion is approximately 125 km (4 degrees of longitude). The inversion does not assume any particular compensation model. If all of the mantle relief were locally compensated by surface topography, a 14.5-km thicker crust in the highlands would have topography elevated by 3 km, while a 14.5-km thinner crust (on average) in the northern lowlands would have 3 km lower topography. This crustal model predicts the known center-of-figure to center-of-mass offset of Mars. Not all of the crustal thickness variation is compensated. The difference between the actual topography (filtered to degree and order 90) and that predicted by the crustal model is shown in Figure 1. This isostatic topography represents the excess (or deficit) relative to locally compensated terrain, much as an isostatic anomaly represents the difference between observed gravity and that of locally compensated terrain.

**Results** The areas shaded in reddish hues have excess topographic loads, such as Tharsis Montes and Alba Patera. Bluish hues represent uncompensated topographic deficits. We find that the linear gravity troughs coincide with up to 2 km of uncompensated topographic relief (green to blue). Such topography also coincides with the steepest portions of the dichotomy boundary (contour). If these regions were buried channels, they would likely be found north and east of the boundary scarps.

**Discussion** The model we propose is that such features were formed in early Martian history during a time of elevated mantle temperature, when the lithosphere was too thin to support uncompensated loads. Erosional modification of

the surface expression of the dichotomy occurred after the crust had cooled significantly and was able to support elastic stresses. There are similar but less pronounced gravity troughs along the edges of Hellas and Isidis, as well as the inferred rim of Utopia. Topographic edge effects of partially compensated relief may be responsible for some of these troughs [6]. Edge effects do not explain the isostatic deficit along steep slopes, and are not the primary reason for the linear gravity troughs.

## References

- [1] D. E. Smith, W. L. Sjogren, G. L. Tyler, G. Balmino, F. G. Lemoine, A. S. Konopliv, The gravity field of Mars: Results from Mars Global Surveyor, *Science* 286 (1999) 94–96.
- [2] F. G. Lemoine, D. E. Smith, D. D. Rowlands, M. T. Zuber, G. A. Neumann, D. S. Chinn, D. E. Pavlis, An improved solution of the gravity field of Mars (GMM-2B) from Mars Global Surveyor, *J. Geophys. Res.* 106 (2001) 23,359–23,376.
- [3] D. N. Yuan, W. L. Sjogren, A. S. Konopliv, A. B. Kucinskis, Gravity field of Mars: A 75th degree and order model, *J. Geophys. Res.* 106(E10) (2001) 23,377–23,401.
- [4] M. T. Zuber, S. Solomon, R. J. Phillips, D. E. Smith, G. L. Tyler, O. Aharonson, G. Balmino, W. B. Banerdt, J. W. Head, F. G. Lemoine, P. J. McGovern, G. A. Neumann, D. D. Rowlands, S. Zhong, Internal structure and early thermal evolution of Mars from Mars Global Surveyor topography and gravity, *Science* 287 (2000) 1788–1793.
- [5] R. J. Phillips, M. T. Zuber, S. C. Solomon, M. P. Golombek, B. M. Jakosky, W. B. Banerdt, R. M. E. Williams, B. M. Hynek, O. Aharonson, S. A. H. II, Ancient geodynamics and global-scale hydrology on Mars, *Science* 291 (2001) 2587–2591.
- [6] A. J. Dombard, M. L. Searls, R. J. Phillips, An alternative explanation for the "buried channels" on Mars: The gravity signal from a sharp boundary on partially compensated, long-wavelength topography, *Geophys. Res. Lett.* 31(5) (2004) L05106, doi:10.1029/2003GL019162.
- [7] G. A. Neumann, M. T. Zuber, M. A. Wieczorek, P. J. P. J. McGovern, F. G. Lemoine, D. E. Smith, The crustal structure of Mars from gravity and topography, *J. Geophys. Res.* in press (2004) 2004JE002262.



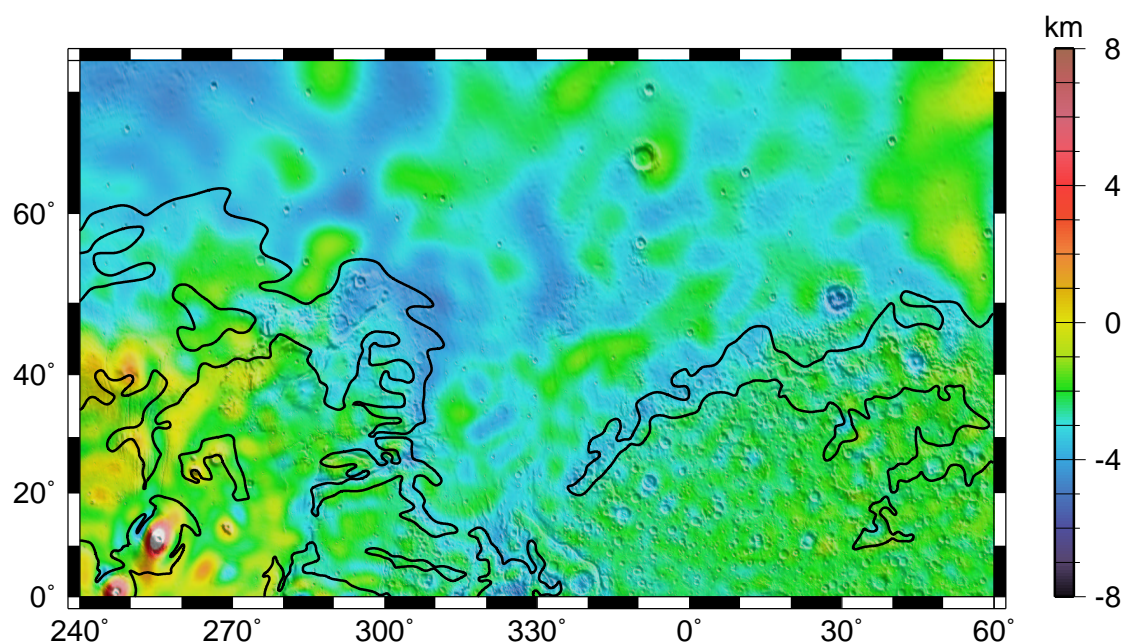


Figure 1: Isostatic topography, the residual topography above that which locally compensates moho relief, in color-shaded Mercator projection. Densities of  $2900$  and  $3500 \text{ kg m}^{-3}$  were assumed for the crust and mantle, respectively. Contours show steeper local gradients of terrain.

**TECTONIC CONSEQUENCES OF DICHOTOMY MODIFICATION BY LOWER CRUSTAL FLOW AND EROSION.** F. Nimmo, Dept. Earth and Space Sciences, University of California Los Angeles, Los Angeles, CA 90095-1567, nimmo@ess.ucla.edu

**Abstract:** The hemispheric dichotomy shows compressional lobate scarps ~100-500 km south of the dichotomy boundary, and extensional features along the boundary itself. Modification of the original boundary by lower crustal flow results in stresses which can explain the origin of both extensional and compressional features. Erosion would lead to extension to the south of the dichotomy, and compression to the north.

**Introduction:** The origin of the Martian hemispheric dichotomy is uncertain [1,2] but its present-day expression is probably due to the crustal thickness being higher in the south than the north [3]. The original surface expression of the dichotomy has been modified by both erosion [4] and impacts [5]. In the Eastern hemisphere of Mars, the dichotomy is characterized by a relatively steep scarp with a gentle rise further to the south. Prominent lobate scarps, interpreted as thrust faults, are found 100-500 km south of the dichotomy, near the crest of the rise [6]. Normal faults are observed along the boundary itself. Note that extensional features further out in the northern lowlands may have been buried by subsequent sedimentary or volcanic deposition. The age of deformation is Late Noachian to Early Hesperian [2,6].

**Lower crustal flow:** As noted by [3] and [7], the dichotomy may also have been modified by the tendency of the lower crust to flow outwards from areas of thickened crust. The rate of flow depends on the crustal thickness, rheology and temperature structure. Figure 1 shows an example of the evolution of the lower crust as a function of time due to lateral flow. Material is redistributed from the thick-crust to the thin-crust side.

The redistribution of lower crustal material will generate loads and thus modify the pre-existing topography. The change in topography depends on the effective elastic thickness  $T_e$  of the lithosphere. (Note that while the lower crustal flow model in Fig. 1 assumes isostasy i.e.  $T_e=0$ , a finite  $T_e$  will have little effect on the behaviour of lateral flow at the wavelengths under consideration here). Fig. 2a shows the final topography caused by the elastic response to the load due to lateral crustal flow. As expected, elevations are reduced on the thick-crust side of the dichotomy.

Fig. 2b shows the resulting surface stresses as a function of  $T_e$ . The reduction in elevation leads to compressional stresses on the thick-crust side of the dichotomy, and vice versa. The timing of the stresses depends on the rate at which lower crustal flow occurs. The lateral extent of the stresses depends on  $T_e$ , which was proba-

bly <15 km during the Noachian [8]. The magnitude of the stresses (~50 MPa) is relatively insensitive to elastic thickness. The corresponding elastic strain is ~0.05%, comparable to the value of 0.2% obtained by [9] from lobate scarp studies. The predictions of compression south of the dichotomy and extension further north are consistent with the observations.

**Erosion:** Erosion is likely to have modified the dichotomy surface topography. Fig 3 shows the effects of erosion, assuming that it can be modelled as a diffusion process. The redistribution of material from high to low elevations results in a load which will cause uplift on the thick-crust side and vice versa.

Fig 4a shows the load resulting from this mass redistribution, and the response of the lithosphere to this load. Isostatic rebound is not complete, because of the finite elastic thickness. Fig 4b shows the resulting surface stresses. The unloading and uplift of the thick-crust side results in extensional surface stresses of up to ~50 MPa. These results are not consistent with the geological observations, and suggest that erosional effects must be outweighed by effects leading to compression, such as lateral flow (see above) or global contraction.

**Discussion:** The mechanism proposed here can explain both the location and magnitude of the observed compressional and extensional features at the dichotomy boundary. It invokes local crustal flow, which is distinct from the global mantle flow models advocated by previous authors [2]. It also differs from the proposal by [6] that surface loading was responsible for the observed tectonic features. If this mechanism is correct, it implies that significant subsurface modification of the original dichotomy boundary has occurred, which will make it harder to test hypotheses of the dichotomy's origin. Conversely, it places limits on how much modification by erosion is likely to have happened.

**References:**

- [1] Frey, H.V. and R.A. Schultz, *Geophys. Res. Lett.* 15, 229-232, 1988. [2] McGill, G.E. and A.M. Dimitriou, *J. Geophys. Res.* 95, 12595-12605, 1990. [3] Zuber, M.T. et al., *Science* 287, 1788-1793, 2000. [4] Hynek, B.M. and R.J. Phillips, *Geology* 29, 407-410, 2001. [5] Frey, H.V. *Lunar. Planet. Sci. Conf.* XXXIII, 1727, 2002. [6] Watters, T.R., *J. Geophys. Res.* 108, 5054, 2003. [7] Nimmo, F. and D. Stevenson, *J. Geophys. Res.* 106, 5085-5098, 2001. [8] McGovern, P.J. et al. *J. Geophys. Res.* 107, 5136, 2002. [9] Watters, T.R. and M.S. Robinson, *J. Geophys. Res.* 104, 18981-18990, 1999.

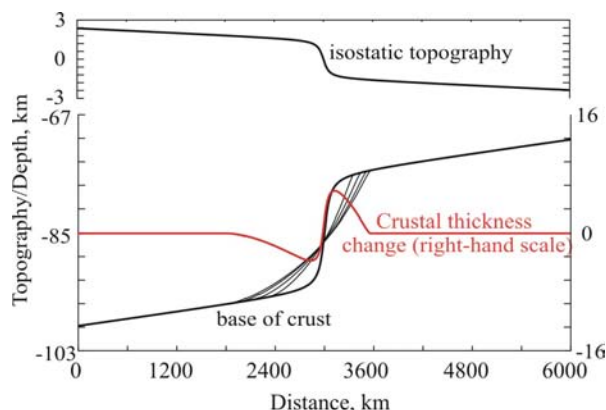


Figure 1. Evolution of crustal thickness with time, using lower crustal flow method of Nimmo and Stevenson (2001). Bold lines depict initial base of crust and resulting isostatic topography. Thin lines show evolution of base of crust with time, due to lateral flow. Red line shows change in crustal thickness; increase in thickness of lower crust generates an upwards load, and vice versa.

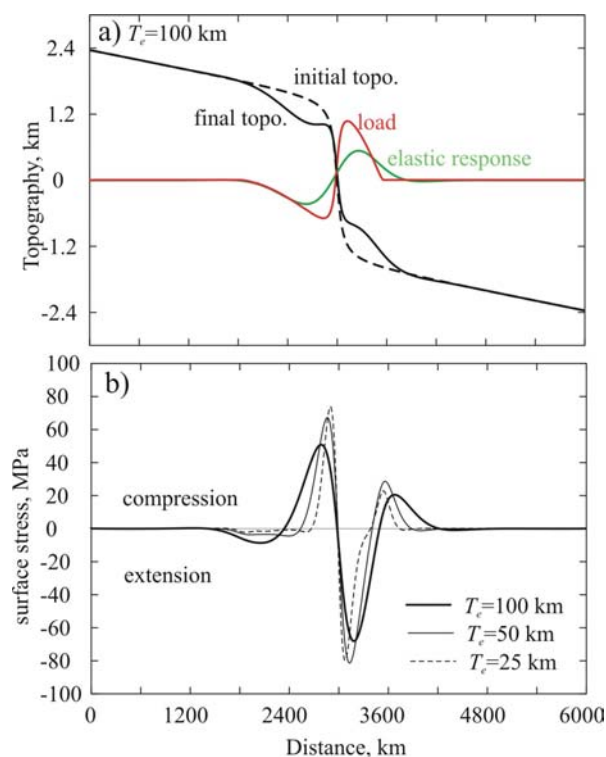


Figure 2. a) Dashed line shows initial topography from Fig 1a. Red line shows load generated by redistribution of lower crust (see Fig 1). Green line shows elastic response ( $T_e=100$  km) to this load. Solid black line shows final topography once the elastic response is taken into account. b) Surface extensional stresses due to load shown in a). Stresses are compressional where crustal thickness has decreased.

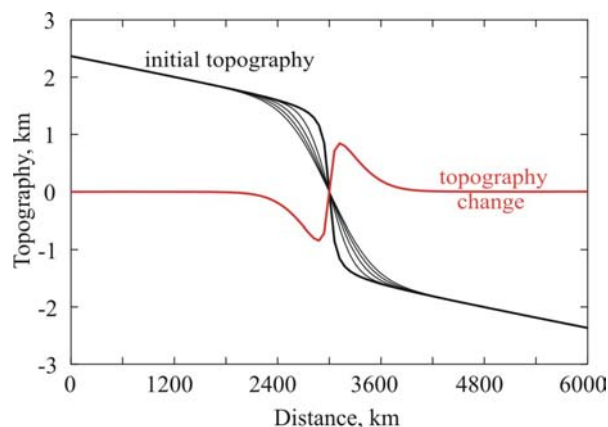


Figure 3. Evolution of topography with time, representing surface erosion by diffusion process. Bold line gives initial topography, red line gives change in topography. Reduction in topography results in an upwards load, and vice versa.

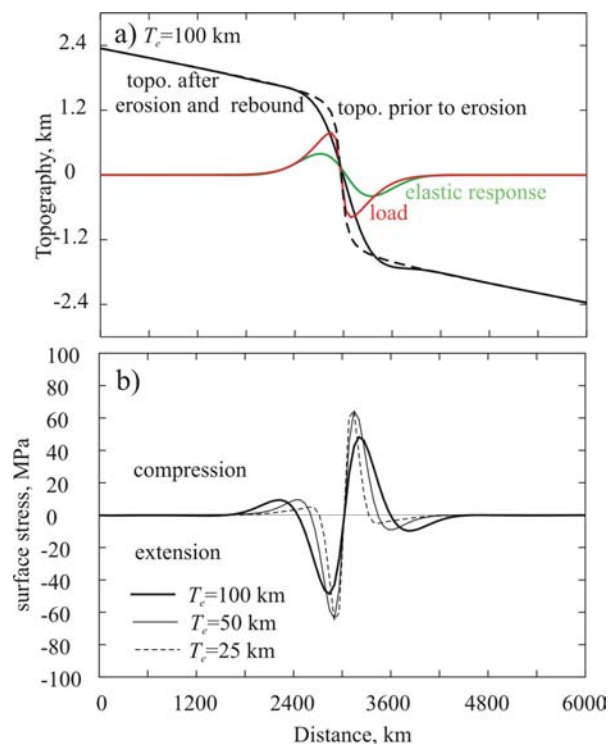


Figure 4. a) Dashed line shows initial topography from Fig 3a. Red line shows load generated by erosion (see Fig 3). Green line shows elastic response ( $T_e=100$  km) to this load. Solid black line shows final topography once the erosional removal of topography and the elastic response are taken into account. b) Surface stresses due to load shown in a). Stresses are extensional where erosion has occurred.

**GLACIAL MODIFICATION OF THE MARTIAN CRUST IN AEOLIS REGION, MARS.** J. Nussbaumer,  
Department of Mineralogy, Natural History Museum, London, UK, [jurn@nhm.ac.uk](mailto:jurn@nhm.ac.uk).

**Introduction:** New Mars orbital data show evidence for widespread glaciation in Aeolis Region (Fig. 1). Geomorphic features like tunnel channels, and drumlins suggest a formation mechanism associated with subglacial high water pressures. Viscous flow features and moraines indicate ongoing sublimation and a rather young age for the retreating ice. These observations complement previous studies that report evidence for glaciation in southern Elysium Planitia.

**Tunnel channels:** Several subparallel broad- and flat-crested branches (Fig. 2a) with steep sides forms a radial and dendritic channel network. They are interpreted as a “tunnel channels”, a subglacial drainage system. Their excavated positive relief (height ~40 m) indicate high pressure sedimentation [1]. The adjacent material was eroded by sublimation or aeolian activity. They are formed by subglacial meltwater flowing under high hydrostatic pressure and have been associated with large subglacial outburst floods on Earth [2, 3]. Sedimentation is thought to have taken place in a waning stage of the flood event, that fills the cavities with stratified sediments. MOLA data shows such crests are oriented perpendicular to the remains of an overlying unit (box in Fig. 1).

**Drumlins:** Longitudinal and streamlined accumulations (Fig. 2a) aligned parallel to former glacier flow directions, are located next to channel like forms and are interpreted as drumlin fields. In special cases, drumlin fields may reflect zones of formation behind former ice margins. Frozen margins could have blocked subglacial drainage, leading to elevated porewater pressures [4]. The general slope according to MOLA data is towards south. Their steep ends point in the up ice direction, the gentler slope is on the lee side. Their formation mechanism is controversial, however it always includes ice sheets. Terrestrial drumlins are concentrated in fields and form where basal shear stress is low and porewater pressures are high [5]. They were associated with catastrophic meltwater floods on Earth [6].

**Viscous flow features:** Sinuous glacier-like flow features, confined by compressional ridges (lateral moraines), are visible in Themis daytime IR images (Fig 3a). Lateral moraines are dumped to the adjacent terrain during ice recession. MOLA data shows a concave U-shaped cross-section which indicates glacial erosion. These flows or former glaciated valleys discharge into a basin showing a bright area in nighttime Themis IR images, indicating higher thermal inertia, suggesting the existence of solid surface material, which maintains day temperatures.

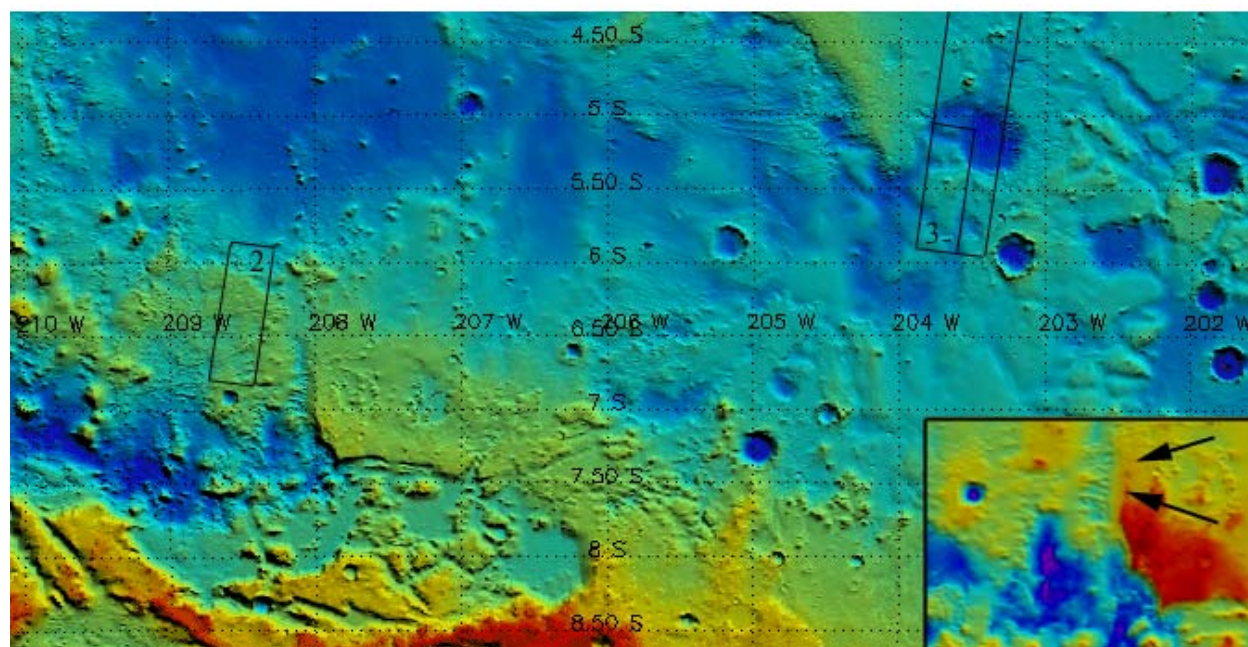


**Fig. 1:** MOLA Overview (128 x 256 pxl/deg.), boxes mark Fig. 2 (left) and Fig. 3 (right), image width is ~500 km, North is up.

**Moraines:** Sinuous lobate ridges are superposed on hummocky terrain, resembling the shape of nearby

higherstanding knobby deposits. These features are interpreted as end moraines and ground moraines, visi-



ble in Themis VIS images (Fig 3b). End moraines as a result of retreating ice are produced by dumping of debris, where the ice margin remains stationary during debris accumulation. Surficial features like round knobs may indicate ongoing sublimation processes. Ground moraines form hummocks and hills and represent the end products of debris-mantled ice ablation [7].

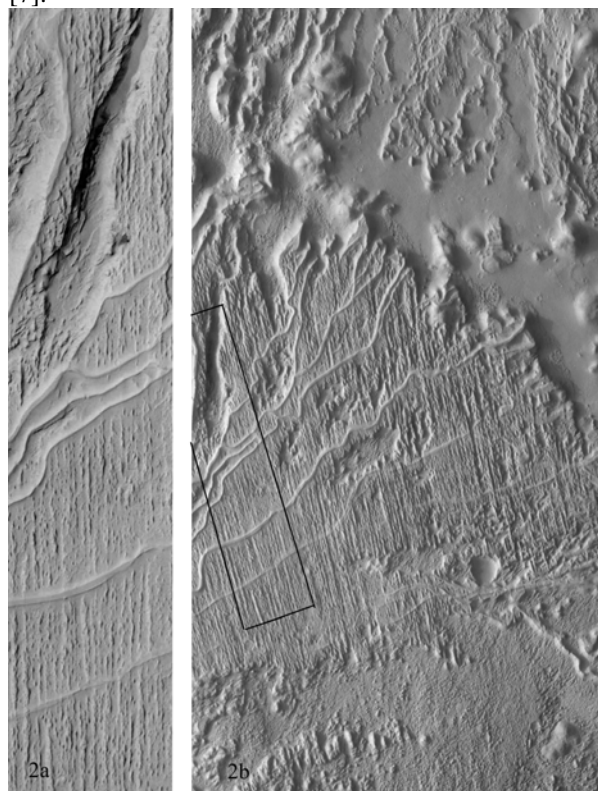


**Fig. 2a:** MOC e1800307 (left), 5,96 m/pxl, ~3km width, Tunnel channels and Drumlin fields.

**Fig. 2b:** Themis V05588002 (right), ~20 m/pxl, 18,4 km width, context image for Fig. 2a, shows branched channels.

**Conclusions:** The formation of equatorial ice sheets is essentially based on two different theories. Firstly, changes of Mars' tilt axis could be responsible for ice deposition in lower latitudes [8]. Secondly, water eruption from pressurized aquifers as a result of a growing cryosphere could form ice sheets as well [9]. Drumlin fields adjacent to tunnel valleys represent erosional forms associated with high water pressures [6]. Terrestrial analogies are found in permafrost regions, where freezing and pressurization of confined aquifers creates pingos and icing outbursts, also existent as cryovolcanism on icy moons.

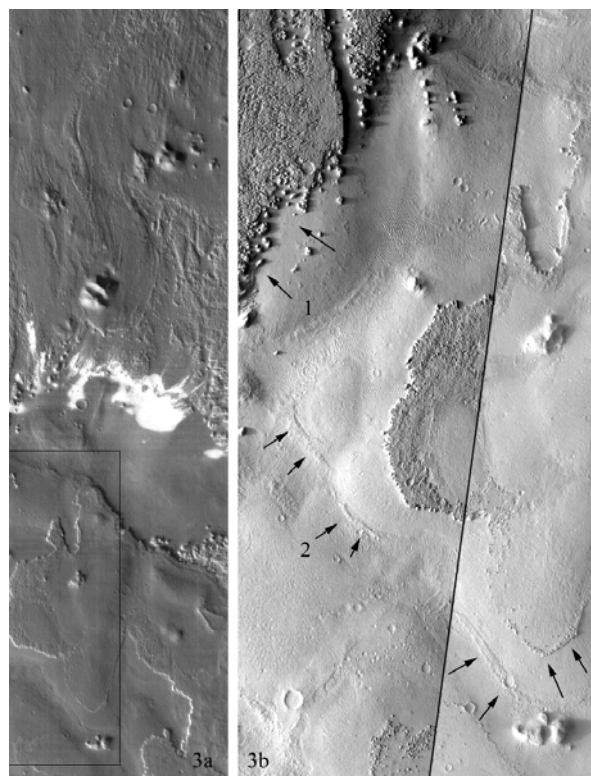


**Fig. 3a:** Themis I07684014 (left) showing Glacier-like viscous flows debouching into a bright basin, image width is 32 km, ~100m/pxl, box marks position of Fig. 3b.

**Fig. 3b:** Themis V06212002, V06574001(right), width is ~20 km, 20m/pxl res., shows moraine-like features (2), hummocky and knobby terrain (1) indicating ongoing sublimation.

#### References:

- [1] Russell, H. A. J. (2003) *Sedimentary Geology*, 160, 33–55. [2] Cutler, P. M. (2002) *Quaternary International*, 90, 23–40. [3] Beaney, C. L. (2002) *Quaternary International*, 90, 67–74. [4] Wright, H. E. (1957) *Geografiska Annaler* 39, 19–31. [5] Patterson, C. J. and Hooke, R. Le B. (1996) *Journal of Glaciology*, 41, 30–38 [6] Shaw, J. (2002) *Quaternary International*, 90, 5–22. [7] Harker, A. (1901) *Transactions of the Royal Society of Edinburgh*, 40, 221–225. [8] Mischna, M. et al. (2003) *J. Geophys. Res.*, 108, E6, pp. 16–1. [9] Gaidos, and Marion, G. (2003) *J. Geophys. Res.* E6 108, pp. 9–1.

**Acknowledgements:** This work is funded by the Marie Curie Association.

**DEGREE-1 MANTLE CONVECTION AS A PROCESS FOR GENERATING THE MARTIAN HEMISPHERIC DICHOTOMY.** James H. Roberts, *Department of Astrophysical and Planetary Sciences, University of Colorado, Boulder CO 80309-0391, USA, (jhr@anquetil.colorado.edu)*, Shijie Zhong, *Department of Physics, University of Colorado, Boulder CO 80309-0390, USA, (szhong@spice.colorado.edu)*.

### Introduction

The crustal dichotomy is one of the most significant topographic and tectonic features on Mars [1]. The gradual pole-to-pole crustal thickness variations inferred from MGS topography and gravity data do not seem to support an exogenic origin, such as giant impacts [2]. We therefore seek to explain this as an endogenic feature, resulting from a degree-1 convection pattern in the mantle [3, 4].

We propose and test two hypotheses for how degree-1 mantle convection may lead to the crustal dichotomy [4]. In the first scenario, the planet starts with no crust at all. Partial melt occurs in a degree-1 plume, where upwelling material is above the solidus. This melt is then extracted to form crust above the plume. In the second scenario, a uniform crust overlies a mantle containing a single convection cell. The Martian crust is thought to be at least 50 km thick [3]. Early in Martian history, the base of such a thick crust may have been so warm as to be ductile. An upwelling mantle plume would erode the lower crust above it and move it laterally to be deposited at the base of the crust above the downwelling. As the interior cools, the crust would lose its mobility and this degree-1 pattern would be frozen in.

For either hypothesis to be tested, it is first necessary to have degree-1 convection in the mantle. We modeled stagnant lid convection in a primitive mantle to test the first hypothesis. In the second scenario, the warm, ductile lower crust may be decoupled from the mantle. The mantle is thus warm enough to be in the mobile-lid regime and we model it as such, overlain by a uniform crustal layer. We used finite-element convection code to solve the equations of mass, momentum, and energy in 2D axisymmetric and 3D spherical geometry [5,6]. The mantle was heated both from below and within and cooled from above. The viscosity was both temperature and pressure-dependent, following an Arrhenius Law. We used non-Newtonian activation parameters appropriate for a wet mantle [7] scaled to Newtonian rheology. We used depth-dependent thermal expansivity and diffusivity and considered the effects of adiabatic and frictional heating [8].

### Stagnant-lid Convection in a Primitive Mantle

Many studies have been done to generate degree-1 convection in a stagnant-lid mantle [4,9-11], but all of them rely upon certain assumptions which may not be reasonable for a general Mars model. We sought to test these mechanisms while relaxing the assumptions to develop a more robust model of degree-1 convection.

Zhong and Zuber [4] achieved degree-1 convection using a layered-viscosity model, with an upper mantle 500 times less viscous than the lower mantle, capped by a high viscosity lid. The viscosity jump is a proxy for various possible mechanisms

including melting, phase change, pressure-dependent viscosity and non-Newtonian rheology. They did not attempt to seek minimum required viscosity jump for degree-1 convection. We wanted to relax the assumption that the mantle was layered, so we attempted to run their model using temperature and pressure-dependent viscosity in place of the layering, while preserving the overall viscosity contrast across the mantle. We were able to maintain a degree-1 pattern when we substituted pressure-dependence for much of the layering, but a jump in viscosity between the upper and lower mantle was still necessary. We were able to reduce the jump to a factor of 25 from a factor of 500 (Fig. 1), but could not eliminate it entirely and still maintain the convective pattern.

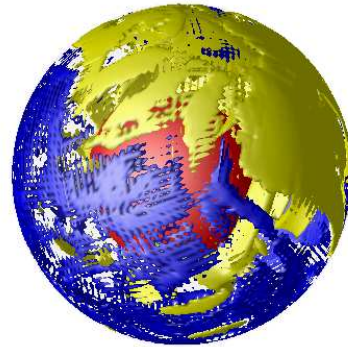


Figure 1: Degree-1 thermal convection pattern from a case with temperature- and depth-dependent rheology and a factor of 25 viscosity jump between the upper and lower mantle. Shown are 5% isosurfaces of residual temperature (yellow: relatively hot, blue: relatively cold)

Several studies [9-11] have utilized phase changes in the mantle as a mechanism for generating a degree-1 convective pattern. Harder and Christensen [9] and Harder [10] considered the endothermic spinel-perovskite phase change in an isoviscous mantle with a high viscosity lid. We successfully reproduced their results in 2D axisymmetric geometry, however, the inclusion of temperature-dependent viscosity destroys the single plume structure (Fig. 2). We have computed models with different phase change parameters, Rayleigh numbers and rheological parameters. We find that only when activation energy is unreasonably low ( $\leq 60$  kJ/mol) we could produce degree-1 convection with the endothermic phase change. Furthermore, recent studies on the size of the Martian core [12] cast doubt as to whether the required pressure for this phase change is ever reached in the Martian mantle. Breuer *et al.* [11] considered the exothermic olivine-spinel transition, including the latent heat effects and obtained a single plume structure. Our experiments with this phase change failed to

produce a degree-1 pattern, indicating the limited role of the latent heating from the exothermic phase change. However, as Harder [10] pointed out, the calculations in [11] are in the mobile-lid regime. This, more than the physics of the exothermic phase change controls the convective pattern. Therefore, it is not surprising that we failed to achieve degree-1 in the stagnant lid regime.

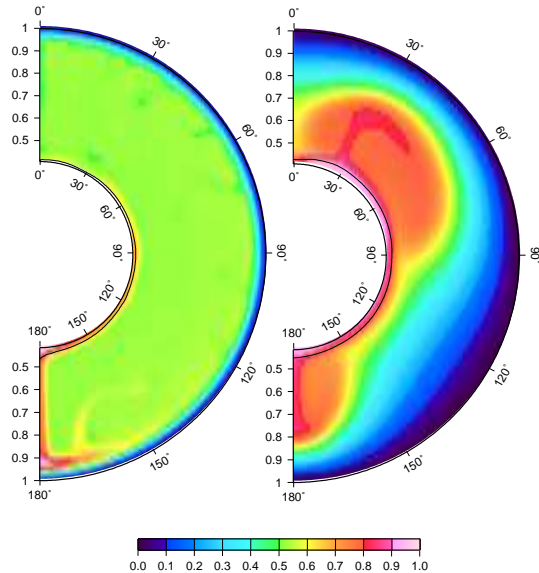


Figure 2: Comparison of two thermal convection cases including endothermic phase change. Location of phase transition indicated by the black curve near the CMB. Left: iso-viscous interior with high viscosity lid. Right: Temperature-dependent viscosity, activation energy of 180 kJ/mol.

### Mobile-lid Convection

Mobile-lid convection, however, may be an appropriate choice for the second scenario. At the time of formation of the hemispheric dichotomy, the lower crust may have been so warm as to be decoupled from the mantle. We ran a series of calculations using the Moho temperature as the upper boundary

condition. The entire mantle was sufficiently warm that the mantle was in the mobile lid regime. However, we have not yet incorporated crust into these models. This produced degree-1 convection in some of the preliminary 2D models. With 3D spherical models, we achieve degree-1 structure with moderate temperature-dependent viscosity.

### Discussions and Future Work

We find that although there are many ways of generating a degree-1 convective pattern in a stagnant-lid mantle, they rely upon certain assumptions that may not be reasonable for a realistic Mars. A layered viscosity structure is one way to get the desired convective pattern, but the actual mantle viscosity depends on temperature and pressure. If a viscosity jump is employed, there must be a physical reason for such a discontinuity. However a number of mechanisms may lead to a jump in viscosity. The exothermic phase change from olivine to spinel may lead to viscosity layering as often suggested for the Earth's mantle. Non-Newtonian mantle rheology may also be able to produce sharp viscosity transitions because of change in deformation mechanisms. We are currently exploring the roles of non-Newtonian rheology in producing sharp viscosity changes.

The mobile lid regime may be appropriate if the crust and mantle are sufficiently warm as to decouple the crust and the mantle, as one may expect for the early Mars. However, care must be taken to couple the convection models to the crustal conduction profile in a physically realistic way. We are currently working on a way to resolve this issue.

### References

- [1] Smith et al. (1999) *Science* 284, 1495. [2] Zuber et al. (2000) *Science* 287, 1788. [3] Wise et al. (1979) *J. Geophys. Res.* 84, 7934. [4] Zhong and Zuber (2001) *Earth Planet. Sci. Lett.* 189, 75. [5] Zhong et al. (2000) *JGR* 105 11063. [6] Moresi and Solomatov (1995) *Phys. Fluids* 7, 2154. [7] Karato and Jung (2003) *Phil. Mag.* 83, 401. [8] Christensen and Yuen (1985) *J. Geophys. Res.* 90, 10,291. [9] Harder and Christensen (1996) *Nature* 380, 507. [10] Harder (2000) *Geophys. Res. Lett.* 27, 301. [11] Breuer et al. (1998) *GRL* 25 229-232. [12] Yoder et al. (2003) *Science* 300, 299.



**CONTROL OF EXPOSED AND BURIED IMPACT CRATERS AND RELATED FRACTURE SYSTEMS ON HYDROGEOLOGY, GROUND SUBSIDENCE/COLLAPSE, AND CHAOTIC TERRAIN FORMATION, MARS.** J.A.P. Rodriguez<sup>1</sup>, S. Sasaki<sup>1</sup>, J.M. Dohm<sup>2</sup>, K.L. Tanaka<sup>3</sup>, H.Miyamoto<sup>2</sup>, V.Baker<sup>2</sup>, J.A. Skinner, Jr.<sup>3</sup>, G.Komatsu<sup>4</sup>, A.G. Fairén<sup>5</sup> and J.C. Ferris<sup>6</sup>.<sup>1</sup>*Department of Earth and Planetary Sci., Univ. of Tokyo, 7-3-1 Hongo, Bunkyo-ku Tokyo 113-0033, Japan ([Alexis@space.eps.s.u-tokyo.ac.jp](mailto:Alexis@space.eps.s.u-tokyo.ac.jp), [sho@eps.s.u-tokyo.ac.jp](mailto:sho@eps.s.u-tokyo.ac.jp))*, <sup>2</sup>*Department of Hydrology and Water Resources, Univ. of Arizona, AZ 85721 ([miyamoto@geosys.t.u-tokyo.ac.jp](mailto:miyamoto@geosys.t.u-tokyo.ac.jp), [jmd@hwr.arizona.edu](mailto:jmd@hwr.arizona.edu))*, <sup>3</sup>*Astrogeology Team, U.S. Geological Survey, Flagstaff, AZ 86001 ([ktanaka@usgs.gov](mailto:ktanaka@usgs.gov), [j Skinner@usgs.gov](mailto:j Skinner@usgs.gov))*, <sup>4</sup>*International Research School of Planetary Sciences, Università d'Annunzio, 65127 Pescara, Italy ([goro@irsps.unich.it](mailto:goro@irsps.unich.it))*, <sup>5</sup>*Centro de Biología Molecular, Universidad Autónoma de Madrid, 28049 Cantoblanco, Madrid, Spain ([agfairen@cbm.uam.es](mailto:agfairen@cbm.uam.es))*, <sup>6</sup>*U.S. Geological Survey, Denver, CO, 80225 ([jcferris@usgs.gov](mailto:jcferris@usgs.gov))*.

**Introduction.** Mars is a planet enriched by ground-water [1,2]. Control of subsurface hydrology by tectonic and igneous processes is widely documented, both for Earth and Mars [e.g., 3]. Impact craters result in extensive fracturing, including radial and concentric peripheral fault systems, which in the case of Earth have been recognized as predominantly strike-slip and listric extensional, respectively [4]. In this work we propose that basement structures of Mars largely result from impact-induced tectonism, except in regions that are dominated by magmatic-driven activity such as Tharsis [e.g., 5] and/or possible plate tectonism during the extremely ancient period of Mars e.g., [6]. In many cases, impact-induced faults appear to have been reactivated and/or displaced by subsequent magmatic-driven groundwater-flow and collapse processes [7].

**Fractured impact crater floors:** These features are concentrated in the ancient cratered highlands along the margins of plain regions and within the lightly cratered plains near the canyon system of Valles Marineris [8]. Moats within some of these craters of varying diameters and relative ages surround plateaus and contain broken material (Fig. 1). The moats appear to be restricted to the margins of highly degraded crater rims. Only certain craters in a given region, however, display these characteristics. Schultz and Glikson [8] proposed that modification processes were localized by the impact structures and restricted to the crater interiors. They interpret this to be the result of heat generated by a tabular magmatic intrusion injected beneath the brecciated zone of an impact crater, which raises the temperature of the overlying material. Thawed materials would then subsequently escape through the peripheral fracture system surrounding the crater, or alternatively, a metastable state of liquification could occur, if the material is confined or the rate of thawing exceeds the rate of escape. The collapsed material within a moat marking a highly degraded impact crater rim forms ridges around a central plateau region (Fig. 1B). This suggests that the degradational processes may have been controlled by extensional concentric faults, possibly initiated during the inward collapse of the transient crater walls [4] and/or by concentric fractures produced by the uplift of the crater floor,

possibly resulting from the injection of a tabular magma body beneath the crater floor [8]. The water-enriched source region, which may have contributed to the formation of the features shown in Fig. 1A,B, has been destroyed, suggesting that the formation of the moat may have involved hydrologic processes. In addition, a depression that transects an impact crater (Fig. 1B) forms part of a longer valley, which terminates at the western margin of the Hydaspis Chaos (Fig. 1, V-B). This scenario may be explained by tabular intrusions being injected under crater floors and/or by hydrologic processes controlled by structures within impact craters [8].

**Progressive highland subsidence and collapse:** Rodriguez et al. [9] described the progressive highland subsidence and collapse of the Late Noachian subdued crater unit [10] in Xanthe Terra (Fig. 1). They propose that regional subsidence and collapse resulted from the release of pressurized groundwater in confined caverns. The release of water described in [9] served as an important, previously unproposed source of the water that carved the outflow channels. Terraced terrain marked by both chaotic terrain and channel bedforms (Fig. 2) may also indicate the release of large quantities of water and related collapse. These observations suggest that the plateau material was degraded and removed more efficiently from within craters than from the surrounding country rock (Fig. 3).

**Crater-related fracture networks:** Layered materials are pervasive on Mars [11] and may contain numerous buried impact craters of varying degradational states (Fig. 3). We propose that impact-induced fracture systems dominate the fracture population in the ancient highlands, away from volcano-tectonic regions [7]. Intermingling concentric and radial fracture systems from multiple impact crater events will result in complex crater fracture networks (CFN). Periods of rapid and/or modest surface burial, or periods of lesser bombardment and higher burial, will result in regions with relatively less abundant buried impact crater populations. As a consequence, the CFN will be less developed. On the other hand, heavy bombardment coupled with slow degradation and/or surface burial are expected to result in denser buried crater populations and highly developed

CFN. We propose that the highland plateaus are stratified into zones of variable fracture density. Fractures radial to impact craters will tend to converge near the buried craters' interior deposits. Since heat flow is hydrothermally transferred more rapidly and effectively along fracture planes, a consequence of this scenario is that pulses of heat, generated by magmatism, for example, will result in a highly anisotropic heat flow distribution, with higher heat flow and thus warming in areas of high fracture density. Valley networks dissecting the crater rims in the ancient highlands [1] suggests that crater interior deposits may have contained significant amounts of water-laden sediments. Therefore, buried impact craters are likely to be ice-enriched regions within the Martian permafrost [2]. Warming of the crater interior deposits might have resulted in melting of large volumes of water and intensive hydrothermal circulation and fracture enlargement, forming conduits that allowed subsurface distal migration of volatiles as well as escape to the surface. We propose that circulation within densely fractured regions will be highly effective at removing crater materials, possibly forming cavities, and resulting in the storage of large amounts of water within the subsurface conduit systems and porous media. Lateral interconnection will be enhanced by subsequent impacts. For example, impacted-induced basement structures and uplifted and overturned strata that dip away from the crater will interconnect regions with different permeability and volatile content. We propose that the distinct topographic levels visible in the plateau region of Fig. 2 can be explained by the successive collapse of densely fractured zones. The distribution of moderately vs. highly fractured zones, particularly if stratigraphically controlled, will determine the number of collapsed plateau levels in a given highland region. If collapse occurs to great depths, or the thickness of the collapse region is relatively thick, the plateau surface might respond by simple crustal warping and fracturing. On the other hand, if collapse occurs to shallow depths or the thickness of the collapse region is relatively thin, chaotic material may result. Evidence such as truncated impact craters preferentially preserved at distinct levels of subsidence (Fig. 2) and collapse features more common on crater floors (versus surrounding plateau material; Fig. 1) collectively add credence to our hypothesis that suggests preferential removal of subsurface crater interior deposits. Yet fracturing and collapse of crater floors were not localized to individual impact structures. Non-uniform groundwater and heat flow may explain why only certain craters display the characteristics described above for a given region. The formation of moats encompassing crater infill (e.g., Fig. 1) suggests that impact-induced fractures are more densely packed around the periphery of the crater rather than beneath the central fill.

**Highland-lowland dichotomy:** The highland-lowland transition regions are marked by a wide range of features indicative of subsidence and collapse. We propose that CFN may have been an important basement control on the lateral and vertical distribution of these topographic variations along the dichotomy boundary.

**Fig. 1.** *A.* THEMIS day-time infrared composite. 50 km in diameter impact crater with a moat around a central plateau (CA). North is at top. Lobate features (L). Impact crater with poorly developed moat (red arrow). A 30 km wide, 300 m deep depression transects the crater (blue pointer). *B.* Composite of MOLA DEM containing *A.*

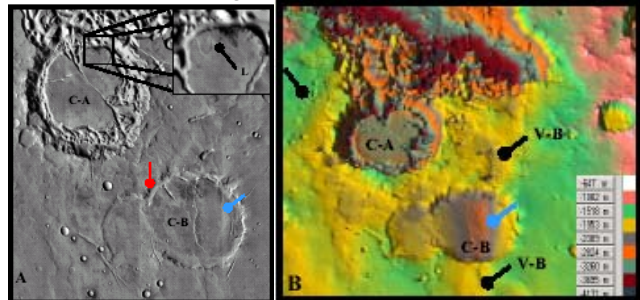
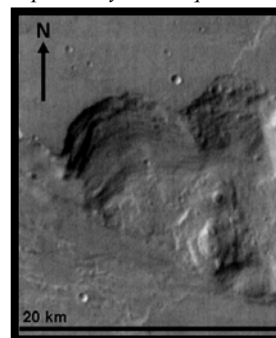


**Fig. 2.** MOLA based DEM. Image is 350 km wide. Noachian plateau region located to the north of Eos Chasma. Chaotic materials occur at several topographic levels (CL-A to E). Channel bedforms (blue arrows). Arcuate scarps (red pointers).



**Fig. 3.** THEMIS day-time infrared subframe showing Noachian plateau near Hydaspsis Chaos. Arcuate scarp 1000 m high exposes layered sequence.



**References:** [1] Carr M.H. (1996) Water on Mars, Oxford Uni. Press. [2] Clifford S.M. (1993) GRL, 19073-11016. [3] Rodriguez J.A.P. et al. (2003) GRL 30, 1304. [4] Osinski G.R. and J.G. Spray (2003) Workshop on Impact Cratering., #8010. [5] Anderson, R.C. et al. (2001) JGR 106, 20,563-20,585. [6] Baker, V.R. et al. (2002) Geosciences 7. [7] Dohm, J.M. et al. (2001) JGR. 106, 32,943-32,958. [8] Schultz H.P. and Gliklen H. JGR (1979) 84, . [9] Rodriguez J.A.P. et al (2004) LPSC XXXV, #1676. [10] Rotto S. and Tanaka K.L. (1995) USGS Map I-2441. [11] Malin M. C. and Edgett K. S. (1999) Fifth International Conference on Mars., #6027.

**OUTFLOW CHANNEL SOURCES, REACTIVATION AND CHAOS FORMATION, XANTHE TERRA, MARS.** J.A.P. Rodriguez<sup>1</sup>, S. Sasaki<sup>1</sup>, J.M. Dohm<sup>2</sup>, K.L. Tanaka<sup>3</sup>, H.Miyamoto<sup>2</sup>, V.Baker<sup>2</sup>, J.A. Skinner, Jr.<sup>3</sup>, G.Komatsu<sup>4</sup> and A.G. Fairén<sup>5</sup> and J.C. Ferris<sup>6</sup>:<sup>1</sup>*Department of Earth and Planetary Sci., Univ. of Tokyo, 7-3-1 Hongo, Bunkyo-ku Tokyo 113-0033, Japan ([Alexis@space.eps.s.u-tokyo.ac.jp](mailto:Alexis@space.eps.s.u-tokyo.ac.jp), [sho@eps.s.u-tokyo.ac.jp](mailto:sho@eps.s.u-tokyo.ac.jp))*,<sup>2</sup>*Department of Hydrology and Water Resources, Univ. of Arizona, AZ 85721 ([miyamoto@geosys.t.u-tokyo.ac.jp](mailto:miyamoto@geosys.t.u-tokyo.ac.jp), [jmd@hwr.arizona.edu](mailto:jmd@hwr.arizona.edu))*,<sup>3</sup>*Astrogeology Team, U.S. Geological Survey, Flagstaff, AZ 86001 ([ktanaka@usgs.gov](mailto:ktanaka@usgs.gov), [jkskinner@usgs.gov](mailto:jkskinner@usgs.gov))*,<sup>4</sup>*International Research School of Planetary Sciences, Università d'Annunzio, 65127 Pescara, Italy ([goro@irsps.unich.it](mailto:goro@irsps.unich.it))*,<sup>5</sup>*Centro de Biología Molecular, Universidad Autónoma de Madrid, 28049 Cantoblanco, Madrid, Spain ([agfairen@cbm.uam.es](mailto:agfairen@cbm.uam.es))*,<sup>6</sup>*U.S. Geological Survey, Denver, CO, 80225 ([jcferris@usgs.gov](mailto:jcferris@usgs.gov))*.

**Introduction:** The formation of outflow channels is classically attributed to the catastrophic discharge of groundwater [e.g.1,2]. Documented modes of confinement and release of groundwater, trapped within the Martian cryosphere include: catastrophic release of groundwater from confined aquifers [3], both catastrophic and non-catastrophic release of groundwater segregated from the permafrost into confined caverns [4], and catastrophic release of groundwater extracted from the permafrost by thermal convection [5]. Multiple events groundwater release resulted in the collapse of plateau materials [3,6,7], and the formation of chaotic terrains, which are mostly located at the head source regions of the outflow channels [6]. Crater counting of the outflow channel floors indicates a late Hesperian age [8], though earlier channeling events may have occurred [8,9,10,11]. Based on geologic mapping and geomorphic assessment using Viking-, Mars Global Surveyor-, and Mars Odyssey-based information of a highland region located east of Valles Marineris and bounded to the south, west, and north by Aureum, Hydraotes, and Hydaspsis Chaos, respectively (hereafter referred to as the subsided plateau region--SPR; Figure 1), we propose new hypotheses, which can potentially explain the following unresolved issues: (1) sources for the large volumes of water required to carve the outflow channels, (2) mechanisms of outflow reactivation, which do not involve recharging of the head source region, and (3) an alternative mode of formation for chaotic terrains.

**Highland subsidence:** The SPR consists mostly of Late Noachian smooth to undulatory intercrater plains materials (unit, Npl2), which are marked by partly buried, mostly rimless and flat-floored impact craters [5]. The surface of the SPR is transected by northwest- and east-trending valley systems (E.G.: Figure 1, V-A). The contact with adjacent regions of the subdued cratered unit is gradational in places and sharp in others (Figure 1, SC, GC). Considerable changes in elevation occur over relatively short distances at contacts. For example, a maximum elevation difference of 2 km over a distance of 100 km is observed at the sharp boundary between SPR and the floor of valley A (Figure 1, SC, V-A). In the western part of valley-A (Figure 1, V-A), linear shallow scarps, (Figure 2B, S), scarp-bounded valleys (Figure 2B, V), and Graben-Horst systems (Figure 2B, GH) are visible. We propose that these features are the

manifestation of different degrees of relative displacement along normal fault planes, which possibly resulted due to ground subsidence [12].

**Post-outflow chaotic terrains:** South of the Hydaspsis Chaos, the surface is heavily fractured with abundant scarps and graben systems in the northern region of the SPR. In this region the plateau margin breaks up gradually into chaotic material (Figure 3). The chaotic material clearly overlaps the surface of the outflow channel (Figure 3), which implies that it, at least in part, post-dates the surface of the adjacent outflow channel. These observations are not fully consistent with a strictly genetic association between chaotic regions and the outflow channels [e.g. 3, 6, 8], in which collapse of the ground formed the chaos, as water and debris were released catastrophically to form the associated outflow channels. Chaotic material possibly resting on top of outflow channel floors may result from aquifer discharges from levels above pre-existing channel floors.

**Evidence for outflow reactivation:** Elevation profiles of channel floor remnants (Figure 1, RM-A, B, C) taken from MOLA data reveal that these regions have the same maximum and minimum elevation values. These regions also display similar geomorphic characteristics and interpreted to result from contemporaneous surface flow activity during early and intermediate stages of excavation of the outflow channels [8]. A northern branch from the Hydraotes Chaos (Figure 1, HB-1) crosscuts the channel floor remnant C (Figure 3). Topographic and crosscutting relationships indicate that two more Hydraotes branches formed subsequently (Figure 1, HB-2, 3). The latest branch is in turn intercepted by the Tiu Vallis lower channel floor (Figure 1, TLC), as indicated by a marginal scarp contact. These observations indicate that reactivation of the flow from the Hydaspsis source region has taken place.

**Discussion:** Our observations indicate that the warped and densely fractured surface of SPR resulted from ground subsidence. Ground subsidence possibly resulted from compensational sinking due to the removal of underground geologic materials by subsurface flow and/or by igneously induced segregation of the water phase within the permafrost into discrete regions, which was subsequently released to the Martian surface. In both cases, in multiple underground levels of caverns



[13] are likely to result. Subsurface structural control, which is consistent with the existence of caverns, is supported by well-defined SPR boundaries and geometric patterns of ground subsidence and collapse features that mimic the trends of adjoining valley systems and basement structures. In the vicinity of the Hydaspiis Chaos region, for example, the SPR is highly fractured, interpreted here to mark collapse of unstable regions of the SPR margin; the formation of the chaotic terrain postdates both the stage of plateau subsidence and the excavation of the adjacent outflow channels. In this particular case, we propose the following sequence of events (from oldest to youngest): (1) large volumes of water are locally stored in multiple levels of confined underground caverns [4], (2) subsequent release of water from these confined systems to the Martian surface combines with the transport of water from distal regions within the putative Tharsis aquifer [14] into the cavernous system, possibly routed through subsurface conduits [4] and/or fracture systems [13], and (3) the emergence of floodwaters from the Hydaspiis and other Chaotic regions in the circum-Chryse region carve the outflow channels. The Hydaspiis Chaos is mainly made up of a cluster of collapsed craters (Figure 1, CC). Since the lower elevations of the crater floors represent regions of relatively lower lithostatic pressure over the confined caverns, and the ground is densely fractured beneath the craters, they are regions where deconfinement is more likely to occur. In the proposed geologic scenario, as water drained away from the caverns, sinking and fracturing of the plateau surface would take place due to a decrease in the basal supportive hydrostatic pressure, ultimately resulting in the formation of the SPR. Reconfinement of the system might result from freezing of its surface region. Buildup of the hydraulic head and outflow reactivation might occur if the hydrostatic pressure increases, which could be caused by (1) thickening of the permafrost seal, (2) sinking of the cavern roof and/or (3) thermal heating of the region related to another pulse of Tharsis-driven magmatic activity [e.g., 14]. Reactivation could also be related to the deconfinement of lower cavernous levels as the confining pressure decreases due to the loss of water and debris from overlying preexisting confined caverns. After water fully drains away from the caverns, relatively shallow, late-stage collapse would occur over the unstable caverns with little or no volatile release. We propose that deconfinement of caverns resulted in the formation of extensive chaotic terrains and large-scale subsidence, features which mark the transition from highlands to lowlands, particularly in the eastern circum-Chryse region of Mars.

**References:** [1] Baker V.R. and D.J. Milton (1974) *Icarus*, 23, 27-41. [2] Baker V.R. (1982) *The Channels of Mars*, University of Texas Press, Austin. [3] Carr M.H. (1979) *JGR*, 84, 2995-3007. [4] Rodriguez J.A.P. et al. (2003) *GRL*, 30,

1304. [5] Ogawa Y. et al. (2003) *JGR* 108, 8046. [6] Carr M.H. (1996) *Water on Mars*, Oxford Uni. Press. [7] Lucchitta, B.K. et al. (1994) *JGR* 99, 3783-3798. [8] Rotto S. and K.L. Tanaka (1995) *USGS Map I-2441*. [9] Scott, D. H. (1993) *USGS I-Map* 2208. [10] Nelson, D. M., and R. Greeley, (1999) *JGR* 104, 8653. [11] Scott, D. H., and K. L. Tanaka, (1986) *USGS Map I-1802-A*. [12] Krassilnikov I. et al. (2003) *Vernadsky Microsymposium* 38, #051. [13] Rodriguez J.A.P. et al (2004) *LPS XXXV*, #.11 [14] Dohm J.M. et al. (2001) *JGR* 106, 32,943-32,958.

**Figure 1.** Context MOLA based DEM. North is up. White circle indicates the location of the MOC subframe in Figure 2. White rectangle indicates the location of the THEMIS image subframe in Figure 3. North at top.

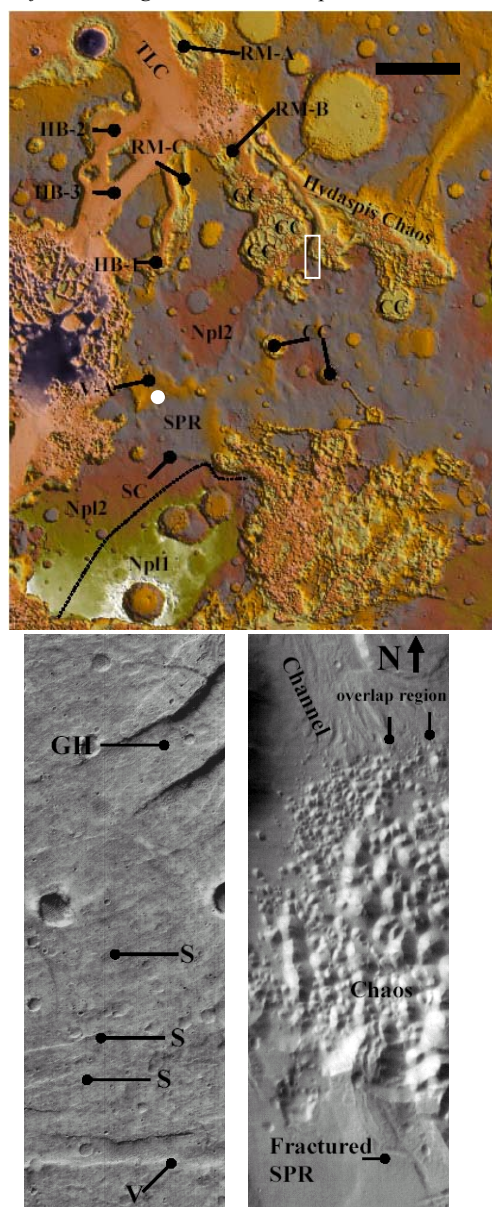


**Figure 2.** (Left) MOCNA image m1800610. Width is 2.77 km. North azimuth is 93. 12° **Figure 3.** (Right) THEMIS day IR 103883003. Width is 32 km. North is up.

**MASS-WASTING OF THE CIRCUM-UTOPIA HIGHLAND/LOWLAND BOUNDARY: PROCESSES AND CONTROLS.** J. A. Skinner, Jr.<sup>1</sup> (jskinner@usgs.gov) K. L. Tanaka<sup>1</sup>, T. M. Hare<sup>1</sup>, J. Kargel<sup>1</sup>, G. Neukum<sup>2</sup>, S. C. Werner<sup>2</sup>, and J. A. P. Rodriguez<sup>3</sup>. <sup>1</sup>Astrogeology Team, U. S. Geological Survey, Flagstaff, AZ 86001; <sup>2</sup>Institute for Geosciences, Freie Universitaet Berlin; <sup>3</sup>Department of Earth and Planetary Science, University of Tokyo.

**Introduction:** Utopia Planitia forms a large (~3300 km diameter), plate-shaped depression interpreted as an ancient impact basin based on its regional gravitational expression [1] and its distribution of knobs, mesas, and partly buried craters [2]. Gravity studies indicate the basin may contain >10 km of material (~50x10<sup>6</sup> km<sup>3</sup>) [8]. The southern and western boundary of the basin is rimmed by a ~400 km wide, arcuate exposure of the highland/lowland boundary (HLB) that extends >4000 km from Nepenthes to Protonilus Mensae (circum-Utopia HLB). The materials generally consist of fractured highland materials, degraded mesas and knobs, interposed slope materials, and smooth to undulating plains. These materials are variably interpreted as marginal marine features [4,5], lava flows [6], mass-wasting materials [2,3], and mud volcanoes [7]. However, these interpretations do not fully address the long-lived modification of the regional HLB and the massive infill of the Utopia impact basin.

We outline observations and offer hypotheses that suggest the circum-Utopia HLB has undergone long-term mass-wasting since the pre-Noachian formation of the Utopia impact basin. These processes are thermally driven, directly affect the ancient structural and stratigraphic framework of the circum-Utopia HLB, appear to be self-propagating, and are able to move massive volumes of material downslope.

**Study Area:** The circum-Utopia HLB was selected because it (1) was likely affected by various levels of geothermal heat, a mechanism to mobilize subsurface volatiles; (2) contains an excellent vertical and lateral exposure of highland and boundary plains materials, generally expressed as subdued “benches” that grade into lowland plains materials; (3) contains both extensional and contractional structural features; and (4) is proximal to a major structural and topographic basin.

**Geologic Character.** The circum-Utopia HLB ranges in elevation from approximately 0 to -3.5 km, though local rises and depressions exist outside of this elevation range. On average, the land surface slopes gently (<1.0°) toward the center of Utopia basin (approx. 50°N, 120°E [2]). However, some scarps, particularly in proximity to the highlands, locally exceed >30°. In general, the circum-Utopia HLB has relatively consistent contact elevations, which grade from cratered highland materials (Noachis unit; 0 to -1

km elevation) to dense knobs, mesas and local depressions (Nepenthes unit 1; ~ -2 km) to smooth, gently undulating plains (Utopia unit 1; -2 to -3 km) and finally, to isolated or coalesced, irregularly-shaped, shallow depressions (Utopia unit 2; -3 to -3.5 km). (Please refer to [3] and [7] for in-depth unit descriptions.) Notable deviations from the above elevation ranges occur in Nepenthes and Protonilus Mensae, where elevations of knobs and mesas are below -2 km. Crater counts indicate the boundary plains materials range in age from Early Hesperian to possibly Early Amazonian, with the youngest surfaces generally residing at the lowest elevations.

**Structural Character.** The circum-Utopia HLB contains both extensional and contractional tectonic features [10]. The most prominent extensional features are normal faults and graben circumferential to Isidis basin (Amenthes and Nili Fossae) that likely represent relaxation of Isidis impact structures. Less well-exposed fractures and graben are located sub-parallel to the HLB within Amenthes Fossae and west of Protonilus Mensae, along a highland massif identified by [2] and associated with the original Utopia impact basin. Though extensional features are currently confined to the higher-standing Noachis and Nepenthes units, subdued linear depressions with correlative trends to adjacent graben are evidence that these features are ancient and once extended through the entire boundary plains sequence. Mass-wasting processes associated with circum-Utopia HLB degradation have obscured these structures.

Contractional features include subdued ridges and broad arches [9], which occur both radial and circumferential to Utopia basin [10]. Radial features are generally prominent to subdued, linear ridges that are most prevalent in Utopia unit 2 while circumferential features are subdued, relatively short arches that are most prevalent in Utopia unit 1. The subdued nature of many contractional features is perhaps a result of poor surface exposure or a general subduing due to erosion or burial [7].

**Hydrologic Character.** Hypotheses that promote a global Martian groundwater table [e.g., 12] are likely inadequate due to the degree of structural development and topographic variability along the hemispheric dichotomy, as such features would impede the interconnectivity of a global aquifer system. Furthermore, recent Martian aquifer modeling by [13] indicates that

local to regional scale processes dominate groundwater migration, leading to relatively short flow paths. As such, we expect circum-Utopia HLB materials to have been affected by groundwater recharge, migration, and discharge via local or regional aquifers. The recharge of upgradient areas may have occurred through highland precipitation during occasional warm periods in the geologic past [14,15]. However, during colder periods when surface volatiles were unstable, external heating and cooling of subsurface volatiles may have driven the circum-Utopia hydrologic cycle. Without recharge, high elevation aquifers would desiccate, and may be susceptible to various mass-wasting processes.

Compared to other regions of Mars, the circum-Utopia HLB is notably lacking in channel-related features, though notable exceptions include the Elysium Fossae-sourced outflow channels [3] and sparse highland valley networks in northwestern Terra Cimmeria [15]. Hephaestus Fossae is the only channel-like feature observed within or immediately adjacent to the boundary plains, and is likely to have formed through groundwater discharge, downslope percolation, and cavernous collapse. While there is general lack of channel features, there is a relative abundance of mass-wasting morphologies and materials.

**Mass-wasting of the circum-Utopia HLB:** Mass-wasting applies to downslope movement of soil or rock under the direct influence of gravity. Such processes may be relatively “wet” (e.g., solifluction) or “dry” (e.g., debris slide). Mass-wasting processes may include ice-lubricated downslope creep, aquifer draining and collapse, mud volcanism-related flows, and slope-instability movements. Since the long-term effect of mass-wasting is planation to a regional base-level, resulting morphologies and materials are often self-destructive and difficult to identify. We note landform and material characteristics of the circum-Utopia HLB that implicate mass-wasting as a major contributor to the modification of the hemispheric dichotomy. Notable observations include (1) boundary plains subsidence related to graben locations, likely as a result of collapse and/or creep processes; (2) surface blisters in boundary materials adjacent to the Elysium rise, likely due to the upwelling of thermally mobilized ground ice; (3) channels and pits of Hephaestus Fossae that are related to groundwater discharge and rapid downslope percolation back into the regolith, possibly across aquifers; (4) lobate depressions of Utopia unit 1, which may have formed via subsidence following aquifer draining or desiccation; (5) small, pitted cones and thin flows occurring in Utopia unit 1, perhaps related to late-stage activity from overpressurized aquifers [7]; (6) the relative smoothness of the Utopia unit 2, perhaps as the result of long-lived downslope proc-

esses; and (7) subdued, chaos-like depressions within Nepenthes and Protonilus Mensae. The latter observation is significant, since the chaos-like morphologies are conspicuously located near the base of highland scarps and are positioned at near-equivalent distances from the estimated center of the Utopia impact basin.

**Implications:** Based on our observations, we offer several hypotheses that outline how mass-wasting has pervasively modified the circum-Utopia HLB since the pre-Noachian formation of Utopia basin. First, circum-Utopia structure and stratigraphy provides a horizontal and vertical framework within which lateral mass-wasting processes may propagate. Ground volatile migration was likely obstructed, and thus concentrated, at such subsurface horizons, many of which may be directly related to the Utopia impact. Second, since regional structure and stratigraphy were likely established early in Mars’ history [16], the degradation of the circum-Utopia HLB was a long-lived, pervasive and self-propagating process that operated at various intensities. Third, mass-wasting intensity was variously affected by interactions between climate and regional geothermal gradients. Thermal effects include both “top-down” effects (those associated with climate variations) and “bottom-up” effects (those associated with endogenic heating). Interplay between these two effects has driven long-term mass-wasting of the circum-Utopia HLB. Fourth, ground volatile migration was regional and resulted from long-term recharge and discharge of local to regional aquifers rather than pole-to-pole hydrostatic pumping [12,15].

**Future Work:** Our careful application and interpretation of crater counts to identify resurfacing events along the circum-Utopia HLB will improve understanding of HLB degradation. We continue to examine top-down (climatic) and bottom-up (geothermal) interactions as they relate to mass-wasting processes and landforms, and plan field studies in high-latitude permafrost and volcanic regions of Earth to examine additional relevant settings and processes.

**References:** [1] Sjogren (1979) *Science*, 203, 1006-1010. [2] McGill (1989) *JGR*, 94, 2753-2759. [3] Tanaka et al. (2003) *JGR*, 108, E4. [4] Parker et al. (1989) *Icarus*, 82, 111-145. [5] Parker et al. (1993) *JGR*, 98, 11061-11078. [6] Wilhelms and Baldwin (1989) *LPSC* 19. [7] Tanaka et al. (2003), *JGR*, 108, E12. [8] Banerdt (2004) *LPSC Abstract* #2043. [9] Watters *JGR*, 93, 10236-10254. [10] Thomson and Head (2001) *JGR*, 106, 23209-23230. [11] Schultz (2000) *JGR*, 105, 12035-12052. [12] Clifford and Parker (2001) *Icarus*, 154, 40-79. [13] Grimm and Harrison (2003) *LPSC Abstract* #2053. [14] Craddock and Maxwell (1993) *JGR*, 98, 3453-3468. [15] Carr (2002) *JGR*, 107, E12. [16] Schultz et al. (1982) *JGR*, 87, 9803-9820

**SUBSURFACE STRUCTURE OF THE ISMENIUS AREA AND IMPLICATIONS FOR EVOLUTION OF THE MARTIAN DICHOTOMY AND MAGNETIC FIELD.** S. E. Smrekar<sup>1</sup>, C.A. Raymond<sup>1</sup>, and G.E. McGill<sup>2</sup>, <sup>1</sup>Jet Propulsion Lab, California Inst. of Technology, M.S. 183-501, 4800 Oak Grove Dr., Pasadena, CA 91109; [ssmrekar@jpl.nasa.gov](mailto:ssmrekar@jpl.nasa.gov); <sup>2</sup>Univ. of Massachusetts, Dept. of Geosciences, Amherst, MA 01003.

**Introduction:** The Martian dichotomy divides the smooth, northern lowlands from the rougher southern highlands. The northern lowlands are largely free of magnetic anomalies, while the majority of the significant magnetic anomalies are located in the southern highlands. An elevation change of 2-4 km is typical across the dichotomy, and is up to 6 km locally [1,2]. We examine a part of the dichotomy that is likely to preserve the early history of the dichotomy as it is relatively unaffected by major impacts and erosion. This study contains three parts: 1) the geologic history, which is summarized below and detailed in McGill et al. [5], this volume, 2) the study of the gravity and magnetic field to better constrain the subsurface structure and history of the magnetic field (this abstract), and 3) modeling of the relaxation of this area (Guest and Smrekar, [6], this volume). Our overall goal is to place constraints on formation models of the dichotomy by constraining lithospheric properties. Initial results for the analysis of the geology, gravity, and magnetic field studies are synthesized in Smrekar et al. [7].

**Geologic History:** Our study area (50°-90°E) is characterized by steep scarps, a fairly rapid change in crustal thickness [3,4], and large magnetic field anomalies in the adjacent lowlands. The area includes a series of 10 graben with slopes of 13° to 21° bounding the rim of the plateau with >3.5% horizontal strain. A topographic bench separates the highlands from the lowlands. The northeastern edge of the bench is defined by the abrupt disappearance of topographic knobs and parallels graben along the dichotomy boundary to the south. These observations support the interpretation that the boundary marks a buried fault, with the lowlands dropped down to the north. Additionally, crater counts indicate that the basement material in the lowlands is likely similar in age to the highlands material [8]. Finally, the 2.5 km of relief at the dichotomy could not have been a result of erosion. Given the similarity in age between the highlands and the bench, erosion would have had to have occurred in the Early Noachian. The scarp separating the highlands and the bench cuts Middle Noachian deposits, and could not have survived early bombardment. Nor could erosion have occurred subsequently as 2.5 km of erosion would have erased all but the largest craters.

**Gravity and Magnetic Field Data:** The free air and Bouguer gravity both have anomalies with a

similar frequency and amplitude variation as that of the magnetic field anomalies. In order to gain more insight into the geologic evolution and subsurface structure in this area, we examine the hypothesis that both the magnetic and gravity anomalies are due to the same source regions. Our modeling of the admittance signature of this area [7] indicates that the highlands regions are isostatically compensated, as is found elsewhere [9-11]. To determine what additional density anomalies remain once both topographic and isostatic effects are modeled, we remove the effect of a 50 km thick crust to produce the isostatic anomaly. Modeling the isostatic anomaly along a profile (50°E, 33°N to 75°E, 49.5°N) perpendicular to the buried fault and dichotomy boundary we find that each of the two main peaks in the isostatic and magnetic field anomalies are offset by approximately 200 km and have a lower peak to the south (Fig. 1). For an intrusion 100 kg/m<sup>3</sup> denser than the surrounding crust, a layer roughly 30 km thick is needed to match the observed gravity anomalies. The more dense the intrusion, the thinner the required layer.

We next model the total magnetic field along the same profile, examining a range of possible paleopole positions consistent with prior estimates [12,13]. In each model the intensity is held constant. The position and thickness of each block is varied to fit the observed data. All of the models in Figure 2 provide a reasonably good fit to the data, except for the model with a 0° paleopole inclination (Fig. 2b). For an inclination of -30°, gaps in the magnetic field are aligned with the locations of the isostatic gravity anomalies (Fig. 2c). For a 30° magnetic inclination (Fig. 2d) the isostatic anomalies are aligned with magnetized crustal blocks.

One possible interpretation of the large positive isostatic anomalies is that they are due to subsurface magmatic intrusions. Both Martian meteorites [e.g. 14] and estimates of volcano densities from gravity studies [9,10,15-17] are consistent with the presence of high-density intrusions. Although no volcanism is visible at the surface, there is a plausible mechanism to produce intrusions in this location. King and Anderson [18] model the effects of a transition in lithospheric thickness on a convecting system and find that localized upwelling is produced at the transition. The extension across the boundary may also be related to the volcanism.



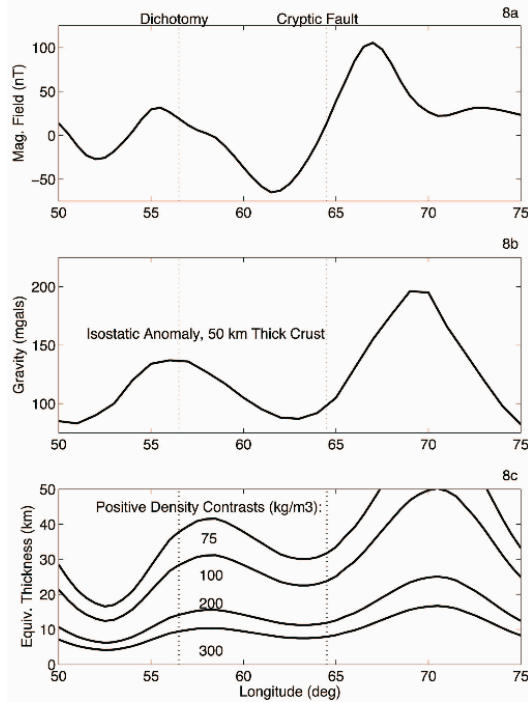


Figure 1. Profiles through the magnetic field (a), and the isostatic gravity anomaly (b), and thicknesses of layers with that would produce an equivalent gravity anomaly (c).

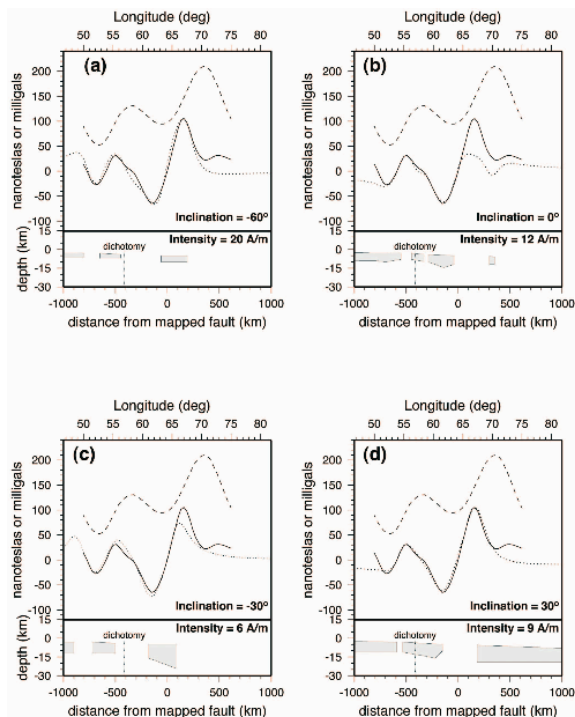


Figure 2. Model fits (dotted lines) to the observed magnetic field in nT (dashed lines) along with the isostatic gravity anomaly in mgals (dashed lines). The source blocks are shown at the bottom of each panel as a function of distance from the buried fault and depth. Intensity and field

inclination assumed for each model are indicated on the figure.

In the magnetic field model shown in Fig. 2c, the gaps in the magnetic field would be caused by magmatic intrusions that both demagnetized the crust and emplaced high-density bodies at depth. An intriguing aspect of this model is that the magnetized crust stops at approximately the location of the buried fault. In an alternate model (Fig. 2d), in which there is a common source for the gravity and magnetic anomalies, the intrusions would have been emplaced in the presence of a magnetic field. An interesting implication of this model is that the plains to the north of the magnetic anomalies are magnetized.

### Preliminary Conclusions and Follow-on Work

The modeling results offer interesting possible interpretations but are non-unique. The next step is to develop a 3D model of the gravity and magnetic field for those anomalies associated with the dichotomy boundary and down dropped block. Objectives include better defining the extent of magnetized material at depth, placing narrower bounds on paleopole position, and determining if there is strong evidence for either correlation or anticorrelation of the gravity and magnetic anomaly source regions. Results will be used to test two alternative hypotheses: 1) magnetic anomalies in the lowlands along the boundary represent highlands crust that has been dropped down via extension across the boundary, and 2) the lowlands are in fact magnetized at a low level. We will continue our study of the dichotomy by examining the geology, gravity, and magnetic field data for additional areas of the dichotomy. Our initial examination of the boundary to the east, in the Amenthes area, indicates a pattern of gravity and magnetic field anomalies with similar magnitude and frequency content.

**Ref:** [1] Frey H.A. et al. (1998) *GRL*, 25, 4409-4412. [2] Smith D.E. et al. (1999) *Sci.*, 284, 1495-1503. [3] Zuber M.T. et al. (2000) *Sci.*, 287, 1788. [4] Neumann, G.A., et al. (2004) *JGR*, in press. [5] McGill G.E. et al. (2004) this conf. [6] Guest, A. & S.E. Smrekar, (2004) this conf. [7] Smrekar et al. (2004), sbmted. [8] Frey (2004) *LPCS XXXV*, Abst# 1382. [9] McGovern P.J. et al. (2002) *JGR* 107, doi: 10.1029/2002JE001854. [10] McKenzie D. et al. (2002) *EPSL* 196, 1. [11] Nimmo F. (2002) *JGR* 107, doi:10.1029/2000JE001488. [12] Cain J. C. et al. (2003) *JGR*, 108, doi: 10.1029/2000JE001487. 1151-1154. [13] Hood L.L. & Zakharian A. (2001) *JGR*, 106, 14601-14619. [14] Britt D.T & G.J. Consolmagno (2003) *Meteor. Planet. Sci.* 38, 1161. [15] Arkani-Hamed (2000) *JGR* 105, 26,712. [16] Kiefer W.S. (2002) Trans. Am. Geophys. Un., Fall Mtg, Abst# P71B-463. [17] Kiefer W.S. (2003) *LPS XXXIII*, Abstract #1234. [18] King S.D. (1998) *EPSL*, 160, 289.

**ENDOGENIC MECHANISMS FOR THE FORMATION OF THE MARTIAN CRUSTAL DICHOTOMY: HYPOTHESES AND CONSTRAINTS.** Sean C. Solomon, Department of Terrestrial Magnetism, Carnegie Institution of Washington, 5241 Broad Branch Road, N.W., Washington, DC 20015 (scs@dtm.ciw.edu).

**Introduction.** The southern uplands and northern lowlands of Mars differ markedly in average elevation [1] and crustal thickness [2,3]. This crustal dichotomy, recognized following the first global observations of the planet by Mariner 9, has variously been attributed to internal [e.g., 4,5] and external [e.g., 6,7] processes, but no single hypothesis for its formation has heretofore been fully persuasive. This paper offers a review of proposed endogenic formation mechanisms for the dichotomy, as well as the geophysical and geochemical constraints [8] that these hypotheses must satisfy.

**Formation Hypotheses.** Excavation and ballistic transport by one [6] or several [7] large impacts have been suggested as an explanation of the crustal dichotomy. Beyond the portion of the dichotomy boundary clearly influenced by the Hellas, Utopia, and Isidis basins, however, there is no confirming evidence from topography for these suggestions [1,2], and no simulations of impacts of such scale have been carried out to test whether the observed pattern of crustal thickness variations [2,3] can be produced.

Endogenic mechanisms proposed for the formation of the crustal dichotomy fall into three classes: those associated with the evolution of an early magma ocean, those associated with an early episode of lithospheric recycling, and those associated with long-wavelength patterns of solid-state mantle flow.

A magma ocean has been postulated as a mechanism to accommodate early differentiation of core, mantle, and crust on Mars and the early establishment of distinct isotopic reservoirs [e.g., 9,10]. The crustal thickness dichotomy may have arisen from the heterogeneous evolution of such a magma ocean during the crustal formation process. Alternatively, crystallization of a magma ocean may have led to gravitationally unstable mantle layering, because the late-stage silicates that crystallized at shallow mantle depths were denser than earlier cumulates that crystallized near the base of the magma layer. Overturn of an unstable mantle may have thickened the crust over downwelling regions and thinned the crust elsewhere [9].

An early episode of lithospheric recycling, or even some variant of plate tectonics, is theoretically possible for Mars [11]. Crust generated at spreading centers at later times might be expected to be thinner than earlier formed crust if the mantle cooled

appreciably during the intervening time, a possible explanation for the crustal dichotomy if the crust of the northern hemisphere is substantially younger than that of the south [11]. If plate recycling was occurring during the formation of the comparatively thicker crust of the southern hemisphere, then such recycling would tend to shut down after the surface area of such crust grew beyond a critical fraction of the planet's surface [12].

Some models of mantle convection, after solidification of any early magma ocean, predict a strongly long-wavelength (harmonic degree 1) component of flow for layered mantle viscosity structures [13]. Such flow models might have led to thicker crust over the hemisphere dominated by upwelling and melt generation, or alternatively thinner crust over that hemisphere if flow-induced crustal thinning was more important than the effect of magmatic additions to crustal volume [13].

**Constraints on Formation.** Hypotheses for the formation of the crustal dichotomy must, of course, account for the present structure of the crust [2,3], as well as the preservation of crustal thickness variations against the tendency of the lower crust to flow in response to stress differences arising from variations in topography at the surface and crust-mantle boundary [2,14]. Any documented differences in major element composition between the crust of the northern and southern hemispheres would be pertinent, but available remote sensing information is subject to multiple interpretations [15,16].

The constraint most able to discriminate among competing hypotheses is the time of formation of most of the crust. A variety of lines of evidence point to crustal formation very early in Martian history, as early as the first 50 My after solar system formation [8].

The most complete simulations of the final stages of terrestrial planet formation to date can account for planets with masses and semimajor axes similar to those of Earth and Venus, but any final body at the orbit of Mars tends to be too large [e.g., 17,18]. While this difficulty may point to an unusually low initial density of disk material in the vicinity of Mars's orbit [17], it may instead indicate that Mars is a surviving embryo that escaped either accretion or ejection [18]. The latter outcome would imply that Mars was nearly fully formed before the final stage of formation of the larger inner planets. Rapid

accretion of Mars would have converted into heat a sufficient quantity of kinetic energy to melt a substantial fraction of the Martian interior and drive global differentiation.

Although surface units in the northern lowlands of Mars are Hesperian to Amazonian in age, numerous partially buried impact craters and basins have been identified from their topographic signatures [19]. Comparison of the density of such features at crater diameters greater than 50 km establishes that the formation of much of the present Martian crust in both hemispheres was complete by the Early Noachian [19].

Isotopic anomalies in Martian meteorites provide strong evidence in support of the inference that global differentiation of core, mantle, and crust on Mars occurred very early in solar system history. The presence of  $^{182}\text{W}$ , a product of the decay of  $^{182}\text{Hf}$  (9-My half life), at levels in all Martian meteorites in excess of that for primitive chondritic meteorites [19-21] is indicative of core formation within 10-15 My of the formation time of the oldest solar system objects [20].

Martian meteorites also contain abundances of  $^{142}\text{Nd}$ , the decay product of  $^{146}\text{Sm}$  (103-My half life), comparable to or in excess of terrestrial values [22]. Nakhilites show elevated levels of both  $^{142}\text{Nd}$  and  $^{182}\text{W}$ , while for shergottites the abundance of  $^{142}\text{Nd}$  varies while the  $^{182}\text{W}$  abundance is approximately constant [23]. These relationships suggest that the source regions for nakhilites were isolated early (while  $^{182}\text{Hf}$  was still extant), whereas the source regions for the shergottites were apparently established while  $^{146}\text{Sm}$  was extant but after all  $^{182}\text{Hf}$  had decayed, i.e., at least 50 My after solar system formation [22].

Several additional lines of evidence support the inference that both the mantle source regions of Martian meteorite magmas and much of the Martian crust were established by 4.5 Ga, i.e., about 50 My after solar system formation. Relationships among isotopes of Pb [24], Sr [25], Os [26], and Nd [27] in Martian meteorites have been interpreted as consistent with large-scale silicate fractionation at about 4.5 Ga and little to no remixing of crust and mantle thereafter. The 4.5-Ga age of ALH84001 [28] also indicates that a stable crust had formed by that time. Such a rapid formation time for the crust and meteorite source regions supports the hypothesis that these regions formed by the differentiation of a global silicate magma ocean that dated from the earliest phase of Martian history [9,10].

A 4.5-Ga age for much of the volume of crustal material on Mars is thus supported by a variety of

indicators, including isotopic systematics of Martian meteorites, expectations from planetary accretion models, and the density of impact craters at the surface and discernible beneath younger infilling deposits. The crustal dichotomy, because of its global scale, must be comparable in age.

**Assessment of Hypotheses.** Plate recycling is probably too slow a process to have formed most of the crust by 4.5 Ga. Hypotheses for the formation of the dichotomy invoking mantle convection patterns subsequent to global differentiation encounter similar difficulties with timescale. An age for most of the crust, including the dichotomy structure, of about 4.5 Ga is most consistent with formation by silicate differentiation of a global magma ocean.

A still open question is the mechanism for producing different average crustal thicknesses on opposite hemispheres by magma ocean differentiation processes. Such an outcome for an early silicate magma ocean is seen on the Moon as well [29, 30], however, and the longest-wavelength crustal thickness variations are those most likely to have survived any early episode of lower crustal flow [2,14].

**References.** [1] Smith D. E. *et al.* (1999) *Science*, 284, 1494. [2] Zuber M. T. *et al.* (2000) *Science*, 287, 1788. [3] Neumann G. A. *et al.* (in press) *JGR*. [4] Mutch T. A. (1976) *The Geology of Mars*, Princeton. [5] Wise D. U. *et al.* (1979) *JGR*, 84, 7934. [6] Wilhelms D. E. and Squyres S. W. (1984) *Nature*, 309, 138. [7] Frey H. and Schultz R. A. (1988) *GRL*, 15, 229. [8] Solomon S. C. *et al.* (submitted) *Science*. [9] Hess P. C. and Parmentier E. M. (2001) *LPS*, 32, 1319. [10] Elkins-Tanton L. *et al.* (2003), *MAPS*, 38, 1753. [11] Sleep N. H. (1994) *JGR*, 99, 5639. [12] Lenardic A. *et al.* (2004) *JGR*, 109, E02003. [13] Zhong S. and Zuber M. T. (2001) *EPSL*, 189, 75. [14] Nimmo F. and Stevenson D. J. (2001) *JGR*, 106, 5085. [15] Bandfield J. L. *et al.* (2000) *Science*, 287, 1788. [16] Wyatt M. B. and McSween H. Y. Jr. (2002) *Nature*, 417, 263. [17] Chambers J. (2001) *Icarus*, 152, 205. [18] Lunine J. I. *et al.* (2003) *Icarus*, 165, 1. [19] Yin Q. *et al.* (2002) *Nature*, 418, 949. [20] Kleine T. *et al.* (2002) *Nature*, 418, 952. [21] Schoenberg R. *et al.* (2002) *GCA*, 66, 3151. [22] Harper C. L. *et al.* (1995) *Science*, 267, 213. [23] Foley C. N. *et al.* (2004) *LPS*, 35, 1879. [24] Chen J. H. and Wasserburg G. J. (1986) *GCA*, 50, 955. [25] Borg L. E. *et al.* (1997) *GCA*, 61, 4915. [26] Brandon A. D. *et al.* (2000) *GCA*, 64, 4083. [27] Borg L. E. *et al.* (2003) *GCA*, 67, 3519. [28] Nyquist L. *et al.* (2001) *Space Sci. Rev.*, 96, 165. [29] Warren, P. H. (1985) *Ann. Rev. Earth Planet. Sci.*, 13, 201. [30] Neumann G. A. *et al.* (1996) *JGR*, 101, 16841.

## TRIGGERING THE END OF PLATE TECTONICS BY FORCED CLIMATE CHANGES.

M. G. Spagnuolo<sup>1</sup>, J. Dohm<sup>2</sup>. <sup>1</sup>Departamento de Geología. Facultad de Ciencias Exactas y Naturales. UBA. [maurospag@yahoo.com](mailto:maurospag@yahoo.com), <sup>2</sup>Department of Hydrology and Water Resources, University of Arizona, Tucson, AZ, 85721 ([jmd@hwr.arizona.edu](mailto:jmd@hwr.arizona.edu))

**Introduction:** Several investigators have suggested that plate tectonics was an active process [1,2], recently proposed for extremely ancient Mars [3-6]. Based on the assumption that accretion and subduction were active processes in the extremely ancient past, and plate tectonism ended in the formation of the southern cratered highlands [7], we propose that the cratered highlands represents a supercontinent that formed through plate tectonism and that it had a significant influence on the subsequent evolution of the planet, which includes catastrophic global climate change. This work brings together some exogenic- and endogenic-derived evidences to propose a new global dynamic model.

**Driving to a Martian Pangea:** Assuming a phase of very ancient plate tectonism, as recorded in the ancient terrains where mountain ranges and other extremely large structures (including fault-controlled basins) [3-5] are recognized, and considering that the presence of magnetic anomalies [8] has been explained either by extensional (probably sea floor spreading) [9] or convergent systems associated with the accretion of oceanic plateaus [3-5], we propose that during lithospheric recycling, which includes the formation of hemispheric dichotomy, a supercontinent was configured. This megacontinent, also known as the southern cratered highlands, should have resulted from accretion of lithospheric plates which is in agreement with a smooth difference in crustal thickness across the dichotomy boundary [10]. The collision of plates also would build up a higher topographic relief in analogous fashion as orogenic belts in Earth.

**A Megacontinent and Its Influence in Global Climate:** After the formation of the Hemispheric dichotomy and emplacement of a Megacontinent, exogenic conditions should have changed dramatically. We propose that the particular geography of this huge supercontinent resulted in catastrophic global climate change. The global climate change would include the development of ice sheets and glaciers due to a higher relief, an associated increase in the planet's albedo, and subsequent global cooling, as has occurred repeatedly in the Earth when supercontinent configurations took place; such supercontinent-related activity has been suggested for a glacial period following the collision of India with Asia (resulting in

the Himalayan rise). Taking into account the smaller size of the planet when compared to the Earth, this self-sustained process of cooling would be of high proportion.

**Cool weather, no water. No water, the end of plate tectonics:** We think that together with fast subduction of hydrated slab peridotite, which removed oceanic water to the interior [3], the increase in the cryosphere caused an initial hydrospheric loss (IHL), where liquid water was removed from the global system. Some authors have suggested that subduction cannot take place in an anhydrous environment due to the absence of silicates, which allows one plate to slide under another one [11]. Eventual planetary cooling (endogenic and exogenic) would result in the termination of plate tectonics around 3.9 [3,4], leaving a supercontinent frozen in time. As plate tectonics transitioned into a stagnant lid (superplume [3,12]) phase of planetary evolution, Mars became less efficient at releasing its internal heat energy, and thus the planet would necessarily heat up [13]. In Earth, supercontinents are unstable and ultimately break into separate plates to allow independent motion [14] following the Wilson cycle. But in Mars, this internal heating and volatile elements, which were added to the interior during subduction [3], would lead to immense episodic outpourings of lava and volatiles such as at Tharsis [15], equivalent of 1.5 bar CO<sub>2</sub> atmosphere and a 120 m thick global layer of water [16]. These MEGAOUTFLO-induced outbursts [3,17] would result in transient climatic, atmospheric, and hydrospheric changes [3,18]

**Conclusions:** The hemispheric dichotomy could be a consequence of a supercontinent formation due to plate tectonics. This established "megacontinent" was responsible for a catastrophic global climate cooling of Mars. This global cooling, together with internal processes, would cause an IHL where liquid water would be removed from the surface. This could favor the end of plate tectonics that preceded an internal heating phase.

References: [1] Sleep N.H. (1994) *JGR*, 99, 5639-5655 [2] Nimmo, F., and Stevenson, D.J. (2000) *JGR*, 105, 11969-11979. [3] Baker, V.R., Maruyama,

S., Dohm, J.M. (2002) *Electronic Geosciences* **7**, (<http://link.springer.de/service/journals/10069/free/conferen/superplu/>). [4] Dohm, J.M. Maruyama, S., Baker, V.R., Anderson, R.C., Ferris, J.C., and Hare, T.M. (2002a) *LPSC XXXIII* abstract 1639. [5] Fairén, A.G., Ruiz, J., and Anguita, F. (2002) *Icarus* **160**, 220-223. [6] Fairén, A.G., and Dohm, J.M. (2004) *Icarus* **168**, 277-284. [7] Lenardic A., Nimmo, F., and Moresi, L. (2004) *JGR*, **109**, E02003, doi:10.1029/2003JE002172. [8] Acuña, M.H. and 13 colleagues (2001) *JGR* **106**, 23,403-23,417. [9] Connerney, J.E.P., Acuña, M.H., Wasilewski, P.J., Ness, N.F., Rème, H., Mazalle, C., Vignes, D., Lin, R.P., Mitchell, D.L., and Cloutier, P.A. (1999) *Science* **284**, 794-798. [10] Zuber, M.T. (2001) *Nature* **412**, 220-227. [11] Ragenauer-Lieb, K., Yuen, D., and Bralund, J. (2001) *Science* **294**, 578-580. [12] Dohm, J.M., Maruyama, S., Baker, V.R., Anderson, R.C., and Ferris, J.C. (2002). *Superplume International Workshop, Abstracts with Programs*, 406-410. [13] Stevenson, D. J., (2001) *Nature* **412**, 214-219. [14] Wilson, J.T., and Burke, (1973) *Eos Trans AGU*, **54**, 238 (abstract) [15] Dohm, J.M., Ferris, J.C., Baker, V.R., Anderson, R.C., Hare, T.M., Strom, R.G., Barlow, N.G., Tanaka, K.L., Klemaszewski, J.E., and Scott, D.H. (2001) *JGR* **106**, 32,943-32,958. [16] Phillips, R. J., Zuber, M.T., Solomon, S.C., Golombek, M.P., Jakosky, B.M., Bandert, W.B., Smith, D.E., Williams, R.M.E., Hynek, B.M., Aharonson, O., Hauck, S.A. (2001) *Science* **291**, 2587-2591. [17] Baker, V.R., Strom, R.G., Gulick, V.C., Kargel, J.S., Komatsu, G., Kale, V.S. (1991) *Nature* **352**, 589-594. [18] Jakosky, B.M. and Phillips, R.J. (2001) *Nature* **412**, 237-243.

**MARS IMPACT ENERGY ANALYSIS IN SUPPORT OF THE ORIGIN OF THE CRUSTAL DICHOTOMY AND OTHER ANOMALIES.** G. R. Spexarth, Representing Self, 14510 Cobre Valley Dr, Houston, TX 77062. spexarth@houston.rr.com

**Introduction:** By analyzing Mars from an engineering perspective, a violent and cataclysmic past is unveiled. This paper looks at multiple anomalies of Mars, shows how they may be inter-related, and describes a very possible scenario, supported by analysis, that could have led to a violent and sudden destruction.

**Impact Energy:** The energy of impact for the 2300 km Hellas Basin, located in the southern hemisphere of Mars, is calculated to be  $5.33 \times 10^{26}$  Joules. This is over 1200 times more energy than the K/T Impact that extinguished 75% of life on earth [1], and Mars is only 1/8 the volume of Earth. This is an enormous amount of energy for Mars to absorb.

This paper shows that the energy input to the Mars system by the Hellas impact is sufficient enough to strain the lithosphere until rupture, thus forming the Tharsis Montes and initiating the Valles Marineris, both of which are located 180 degrees away from the Hellas Basin (Fig-1).

By analyzing the lithosphere of Mars as a thin-wall pressure vessel, it is shown that the amount of energy required to rupture the lithosphere ranges from 36% to 84% of the total Hellas impact energy. This assumes that the lithosphere thickness is between 110-260km [2]. Based on this analysis, there was sufficient energy in the Hellas impact to rupture the planet's lithosphere. Prior to rupture, the lithosphere would deform due to excessive yielding, thus forming the Tharsis Montes.

**Tharsis Montes:** It is proposed that this rupture initiated radial fractures that are identified as originating at the center of the Tharsis Montes (Bulge) [3]. The Tharsis volcanoes and Valles Marineris are aligned 60-degrees radially from each other (Fig-2). It is shown that 60-degree radial fractures (six-sided petals) are a typical feature formed when thin-walled pressure vessels rupture due to a build-up of excessive internal pressure (Fig-3) [4], [5]. These radial fractures could have been the source of extensive volcanism observed in the Tharsis region, as well as the initiation of the Valles Marineris as a rupture in the lithosphere.

**Northern Lowlands:** In addition, the Northern Lowlands are 5 km below datum ("sea level") and the Tharsis Bulge is 10 km above datum [6]. It is proposed that the Northern Lowlands are a direct result of the lithosphere deforming to create the Tharsis Bulge. The increase of arc-length required to form

the Tharsis Bulge is shown to correspond directly to the reduction of elevation and arc-length of the Northern Lowlands.

**Rate of Rotation:** The rotational rate of Mars is slower than predicted when compared to the angular momentum of the rest of the terrestrial planets [7], [8]. It is shown that only 8% to 18% (depending on the thickness of lithosphere assumed) of the total impact energy from the Hellas Basin would be required to reduce the rotational spin of Mars by 20%.

**Magnetic Field:** It is also suggested that this sudden reduction of Mars' rotation, as well as pressure waves originating from the Hellas impact and passing through the possible liquid iron core, would disrupt the rotation of the liquid core, and in turn, significantly affect the dynamo process. Unless specific conditions are met, the planetary dynamo is non-regenerative [9]. Therefore, the planetary magnetic field would remain at a depleted level, and Mars would be in the present state that we find it in today.

**Atmosphere:** Without a magnetosphere to protect the planet from the Sun's solar wind, the atmosphere of Mars would be etched away and blown into space and leave it with the minimal amount of atmosphere that it has today [10].

**Conclusion:** This paper proposes, and provides evidence for, an alternate geological past for Mars. Detailed structural analysis supporting this theory is provided herein. However, ultimately, Mars must be explored in order to unlock its secrets and fully understand the implications of its history.

**References:** [1] Sharpton, V. L. and Grieve, R. A. F. (1990), *Global Catastrophes in Earth History*, pp. 301-318. [2] Willemann, R. J. and Turcotte, D. L. (1982), *JGR*, Vol-87, No. B12, pgs (9793-9801). [3] Carr, M. H., (1974), *Tectonism and Volcanism in the Tharsis Region of Mars*, *Jour. Geophys. Res.*, V. 79, pg 3943-3949. [4] Whitney, J. P. (1993), *NASA-JSC 32294*. [5] Friesen, L. J. (1985), *NASA-JSC 27081*. [6] Cattermole, Peter (1992), *Mars, The Story of the Red Planet*. [7] Mars Orbiter Laser Altimeter (MOLA), NASA/GSFC, <http://ltpwww.gsfc.nasa.gov/tharsis/mola.html>. [8] Chabai, A. J. (1977), *Influence of Gravitational Fields and Atmospheric Pressures on Scaling of Explosion Craters*, *Impact and Explosion Cratering*, pgs. (1191-1214). [9] Russell, C. T. (1986) *Solar and Planetary Magnetic Fields*. [10] Luhmann, Janet G., (1996), *Solar Wind Effects on the Atmospheres of*

*the Weakly Magnetized Bodies: Mars, Titan, and the Moon*, NASA Contractor Report 202224.

[11] Hancock, G. (1998), The Mars Mystery.

### Figures:

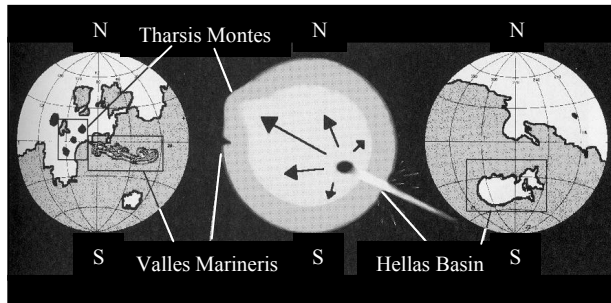


**Figure-1.** Formation of the Tharsis Montes and Valles Marineris due to the Hellas Impact. [11].

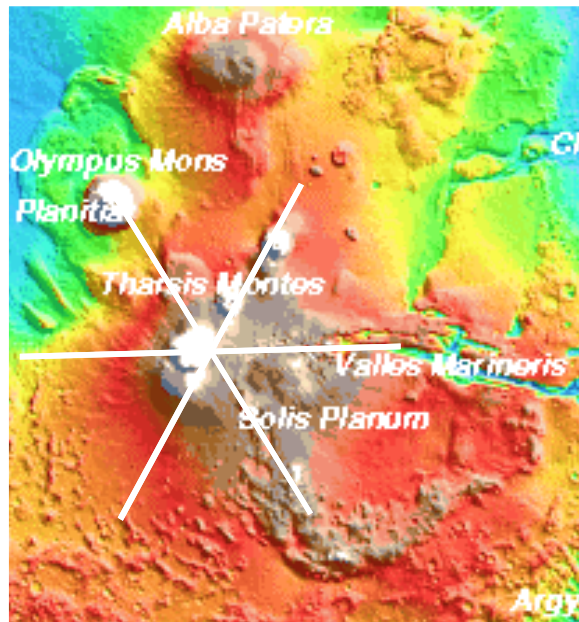


**Figure-2:** Six-sided star pattern observed in the Tharsis region. This pattern is typical during rupture of thin-walled pressure vessels. [7] (radial lines added by author) (formation best observed on color map)



**Figure-3:** Six-sided star pattern observed in the rupture of thin-walled pressure vessels in a laboratory experiment [4], [5].



**TOPOGRAPHIC AND GEOMORPHIC MODIFICATION HISTORY OF THE HIGHLAND/LOWLAND DICHOTOMY BOUNDARY OF MARS: I. NOACHIAN PERIOD.** K.L. Tanaka, Astrogeology Team, U.S. Geological Survey, Flagstaff, AZ 86001; [ktanaka@usgs.gov](mailto:ktanaka@usgs.gov).

**Introduction.** Formation of the Martian hemispheric highland/lowland boundary (HLB) may be the earliest recorded landscape-producing event on the planet [e.g., 1]. The boundary traverses a somewhat sinuous path that encircles about one-third of the planet's surface, separating the -2000 to -6000 m lowlands from highlands that average several thousand meters higher in elevation. The HLB has a regional slope that averages  $\sim 1^\circ$  across a few hundred kilometers [2]; however, it varies in detail from a relatively abrupt scarp (e.g., Isidis, Elysium, and Amazonis Planitiae), to an abrupt top scarp having lower, beveled ledges or benches (e.g., Utopia basin), to a gentle slope (parts of northwest Arabia and northeast Tempe Terrae, and southeastern Elysium Planitia).

Both impact and tectonic origins for the dichotomy remain in vogue to account for the low topography, thin crust, and low remanent magnetization of the northern lowlands [e.g., 3]. Either type of origin likely produced extensive fault and fracture systems and rock units, which have long-since been obscured by subsequent geologic activity. However, ancient, impact-related structure and rock units, perhaps highly altered, may be preserved at depth. Here I discuss the earliest geomorphic modification of the highland/lowland topographic boundary as recorded in the extant Noachian surface geology; a companion abstract describes younger, Hesperian and Amazonian modification.

**Early Noachian impacts.** Among the most profound modifications of the HLB are huge impacts. Utopia basin forms a circular depression about 3300 km in diameter containing a positive free-air gravity anomaly and thin crust consistent with an impact origin [4-6]. However, finer-scaled structures and deposits pertaining to its origin are not clearly recognized. The southern and western margins of Utopia basin account for about one-fourth of the HLB. Curiously, it transitions smoothly into adjacent sections of the HLB north of Arabia Terra and south of Elysium Planitia, so it is unclear whether the formation of Utopia basin had a relatively moderate or substantial effect on the original outline of the HLB.

Another huge impact may account for the broad (nearly 2,000 km across) lowland embayment of Chryse Planitia, which has some poorly preserved indications of a circular basin structure, including massifs along the western basin flank [7]. Isidis basin forms the best-preserved but smallest of the major Early Noachian impacts that have modified the HLB. It forms a basin  $\sim 1200$  km in diameter that partly overlaps the southwest margin of Utopia basin. A broad, low (a few hundred meters high) shoulder separates the basins. Isidis basin preserves a strong positive gravity anomaly [5] and is partly ringed by arcuate troughs (Nili and Amenthes Fossae) and high-standing massifs (Libya Montes).

**Noachian resurfacing.** Mars Orbiter Camera images at high resolution (a few meters/pixel) reveal that the heavily cratered terrain that comprises the oldest, most widespread rocks of the HLB appear to be pervasively layered, where fresher exposures occur [e.g., 8]. The layered highland rocks likely result from a complex history and interplay of geologic processes. Layer origins likely include: (a) thousands of local to regional crater ejecta blankets, (b) blankets of ash and perhaps volcanic flows, particularly in and near the Tharsis rise, which overlies the HLB and began forming in the Noachian [9-10], (c) alluvium and paleolake sediments within inter- and intra-crater plains formed by fluvial dissection of high topography [e.g., 11-12], and (d) eolian dust mantles from atmospheric fallout from dust storms [9, 13]. These deposits may have become mildly to highly consolidated and indurated through compaction and/or chemical cementation. They also may have been saturated or supersaturated with both groundwater and ground ice during or after deposition. Depending on the climatic conditions during the Noachian and local/regional thermal regimes, these widespread aquifers may have resulted in a variety of Earth-like polar/subpolar hydrogeologic settings, such as fluvial, glacial, and periglacial environments. Derived erosional materials could have contributed to sedimentation, particularly along and below the HLB and among massifs such as at Libya Montes and the montes west of Chryse Planitia and Mareotis Fossae. Noachian oceans have also been proposed within the northern lowlands [14], but the geomorphic evidence is not compelling [15-17].

Along with deposition, erosion of the landscape may have been extensive during the Noachian, as evidenced by impact craters in various stages of degradation. Impact gardening no doubt pulverized surface rocks ubiquitously to depths of meters or more depending on the size of impactors, target material properties, and local to regional net rates of resurfacing [18-19]. The comminuted material produced by impacts may have been susceptible to other erosive processes or become trapped in depressions. Potentially, repeated pulverization and grinding of originally intact materials such as igneous rocks, impact melt, and cemented deposits, could have led to an extensive megaregolith a couple kilometers thick over much of the surface [18]. Fluvial erosion of Noachian rocks may have been prominent in many areas and perhaps ubiquitously [20-21]. In some cases, paleolake discharges led to catastrophic floods and deep dissection, such as Ma'adim Vallis [12]. Locally, erosion by mass wasting processes, particularly where ground ice and water were present, may have been extensive.

**Noachian tectonism.** Tectonic modification of the HLB likely resulted from stresses generated by global cooling and contraction and early growth of Tharsis,

which included lithospheric loading [22], upwelling and dynamic support [e.g., 23], and modification of the gravity field [24]. Surface modification would include formation of wrinkle ridges, grabens, normal faults, and alteration of slope-directed erosive processes including fluvial dissection [22, 24, 25]. However, the Early to Middle Noachian tectonic record mostly either is not well preserved or is difficult to isolate from more distinctive, younger structures, many of which may represent rejuvenated, older structures.

**Summary.** Noachian modification of the HLB appears to have been extensive. Gross reshaping took place due to the Utopia impact and a likely Chryse impact. These features may have greatly enlarged the extent of the northern plains by producing embayments reaching across hundreds to a few thousand kilometers in width and breadth. Isidis basin in turn modified the margin of Utopia basin thereby extending a further embayment of lowlands. A variety of resurfacing processes, include impacts, volcanism, fluvial and other erosive processes likely resulted in burial of the primordial crust by a megaregolith that may be kilometers thick. Tectonism likely has affected the HLB to some degree, but much of its record during the Noachian may have been erased or obscured by later activity.

**References.** [1] Frey H.V. (2004) LPSC XXXV, #1382. [2] Frey H.V. et al. (1998) GRL 25, 4409. [3] Nimmo F. and Tanaka K.L. (2005) Ann. Rev. Earth Planet. Sci., submitted. [4] McGill G.E. (1989) JGR 94, 2753. [5] Smith D.E. et al. (1999) Science 286, 94. [6] Zuber M.T. et al. (2000) Science 287, 1788. [7] Schultz P.H. et al. (1982) JGR 87, 9803. [8] Malin M.C. and Edgett K.S. (2001) JGR 106, 23,429. [9] Tanaka K.L. (2000) Icarus 144, 254. [10] Hynek B.M. et al. (2003) JGR 108, 5111. [11] Malin M.C. and Edgett K.S. (2000) Science 290, 1927. [12] Irwin R.P. and Howard A.D. (2002) JGR 107, doi:10.1029/2001JE001818. [13] Haberle R.M. et al. (2003) Icarus 161, 66. [14] Clifford S.M. and Parker T.J. (2001) Icarus 154, 40. [15] McGill G.E. (2001) GRL 28, 411. [16] Tanaka K.L. et al. (2003) JGR 108, 8043. [17] Carr M.H. and Head J.W. III (2003) JGR 108, 5042. [18] MacKinnon D.J. and Tanaka K.L. (1989) JGR 94, 17,359. [19] Hartmann W.K. (2001) Icarus 149, 37. [20] Grant J.A. and Schultz P.H. (1990) Icarus 84, 166. [21] Craddock R.A. and Maxwell (1993) JGR 98, 3453. [22] Tanaka K.L. et al. (1991) JGR 95, 15,617. [23] Kiefer W.S. (2003) Meteorit. Planet. Sci. 38, 1815. [24] Phillips R.J. et al. (2001) Science 291, 2587. [25] Anderson R.C. et al. (2001) JGR 106, 20,563.

**TOPOGRAPHIC AND GEOMORPHIC MODIFICATION HISTORY OF THE HIGHLAND/LOWLAND DICHOTOMY BOUNDARY OF MARS: II. HESPERIAN AND AMAZONIAN PERIODS.** K.L. Tanaka, Astrogeology Team, U.S. Geological Survey, Flagstaff, AZ 86001; [ktanaka@usgs.gov](mailto:ktanaka@usgs.gov).

**Introduction.** Modification of the highland/lowland boundary (HLB) on Mars is a long, complex story involving a large portion of the planet as well as the entire span of recorded geologic history of the planet. The Noachian history is described in a companion abstract and involves much of the first-order form and relief of the HLB and characterization of the materials forming the ancient crust. This abstract addresses how the HLB was subsequently modified during the Hesperian and Amazonian Periods. Recent geologic mapping and topical studies based largely on Mars Orbiter Laser Altimeter elevation data [1] have contributed to new perspectives on this history [e.g., 2].

**End of Noachian to Amazonian HLB erosion and mass wasting.** Modification of the HLB beginning near the end of the Noachian is better preserved in the geomorphologic record than earlier activity. The character of modification varies by region as delineated in the following subsections.

*Utopia basin.* Among the most pronounced HLB modification is the apparent two-level, two-stage degradation observed between Lyot crater and south-southwest of Elysium Mons, except where disrupted by Isidis basin [2, 3]. The upper level ranges mostly from -1800 (or higher) to -2900 m and the lower level from -3100 to -3500 m. South of Lyot crater along the southern margins of Deuteronilus Mensae, the upper, older contact apparently deepens to -3600 m. Upper-level collapse occurred from about the end of the Noachian into the Early Hesperian (N(5)~165), whereas the lower level is Late Hesperian (N(5)~90). Generally, the elevations of these contact levels decrease radially from the center of Utopia basin and may reflect an overall, gradually deepening zone in which undermining and collapse of the Noachian strata took place. Also, local evidence for possible sedimentary volcanism and groundwater discharge of possibly Late Hesperian and Amazonian age indicates local resurfacing within lowland rocks [2-4].

These observations are consistent with stratigraphic control of mass wasting for a giant impact into flat-lying beds. Strata surrounding the crater are gently uplifted and buried near the crater rim by overturned beds and by radially thinning ejecta, resulting in strata that dip away from the impact structure, accounting for horizons in which mass wasting and collapse occur [5]. In addition, the buried substrate may include dense impact fracture networks that could also lead to development of caverns and collapse features [6].

*Chryse basin.* Several sinuous valley systems dissect the highland margins (Xanthe Terra) of Chryse Planitia, which may account for Late Noachian (N(5)~230) deposits as well as middle Hesperian deposits (N(5)~120) on the basin floor [2]. Outflow channel dissection and

deposition and chaos formation generally appears to be Late Hesperian (N(5)~90). This activity could have erased evidence of earlier outflow discharges. Low knobs are plentiful in eastern Chryse Planitia, suggestive of shallow mass wasting during the Hesperian. Similar to Utopia basin, the putative Chryse impact structure may have resulted in strata susceptible to collapse that dip away from Chryse Planitia. This is indicated by the floor levels of chaos, which decrease in elevation from -4100 m at the northern margin of the chaos in Simud Vallis to -5000 m in Hydraotes Chaos, across a radial distance of ~800 km from the margin of the proposed impact basin.

*Northwest Arabia Terra.* Between Chryse basin and Deuteronilus Mensae, Arabia Terra dips gradually into the northern lowlands and includes one to two relatively low boundary scarps generally a few hundred meters high. The Vastitas Borealis Formation (VBF) obscures the HLB below -4000 m. Within Arabia Terra and the VBF, especially in the Cydonia region, sets of irregular collapse depressions disrupt surface materials [2]. The lowland depressions include dense fields of knobs and local, high-standing mesas. The floors of these plains depressions along the HLB decrease in elevation northeastward away from Chryse basin from -3500 m southwest of Mawrth Vallis to -4600 m at Cydonia Colles/Labyrinthus. Nearby depressions in Arabia Terra reach depths of -4900 m. Depressions surrounding Acidalia Mensa, which appears to be a low-lying plateau of Noachian material, bottom out at -4700 to -5000 m. The base elevations of these features also could be related to collapse controlled in part by the Chryse impact-basin structure and strata gently dipping northeastward, and/or to the regional surface slope.

*Tempe Terra.* The northern margin of Tempe Terra forms the northernmost part of the HLB. The eastern margin of this plateau generally slopes gently into Acidalia Planitia and appears to be terraced and extensively graded by fluvial channel systems, probably Late Noachian in age. Collapse structures are not evident, except near Kasei Valles. In contrast, northwestern Tempe has an abrupt margin 1 to 2 km high ringed by a band of large, dispersed knobs that are embayed by flows from Alba Patera. Mareotis Fossae defines the western margin of Tempe and forms rugged plateaus marked by broad troughs, reflecting both extensional tectonics and mass-wasting processes. This margin is proximal to Alba Patera and other volcanic centers, and thus geothermal activity was likely pronounced periodically at Mareotis Fossae.

*Elysium and Amazonis Planitiae.* Much of this part of the HLB is buried and embayed by Amazonian materials, including the Medusae Fossae Formation and lava flows associated with the Elysium and Tharsis rises. The HLB tends to form an abrupt scarp hundreds of meters to

more than a kilometer high, below which Late Noachian to Early Hesperian ridged plains material embays the HLB. The plains material could have diverse origins including volcanic flows, fluvial sediments, or mass-wasting deposits. Farther north, inliers of chiefly Noachian materials and perhaps some ridged plains material crop out extensively as dense patches of knobs and moderately degraded cratered terrain. The scarp is locally dissected by channel systems, including Mangala and Ma'adim Valles. However, a gentle slope and scattered knobs characterizes much of the HLB west of Ma'adim Vallis, with a dense knob field southwest of Apollinaris Patera. Locally, the flows overlying the HLB are marked by grabens generally radial to and wrinkle ridges concentric to Tharsis. Sporadic discharges across and below the HLB formed Mangala Valles and other valley systems west and southeast of the Elysium rise during the Late Hesperian through the Late Amazonian [7].

*Isidis basin.* Three distinct zones of the HLB border Isidis, including the rugged, dissected Libya Montes along the south margin, the gently sloping Syrtis Major Planum consisting of lava flows along the west margin, and the sloping knobby cratered terrain along the north margin. Local collapse structures form along the HLB, including shallow depressions that mark the west and lowest margin of Isidis Planitia. The Early Amazonian VBF deposit that covers the basin floor slopes gently southwestward and has been attributed to tectonic tilting in response to loading in the northern plains [8].

**Amazonian subpolar modification.** Following emplacement of the VBF, a large section of lowlands north of Alba Patera appears to have been degraded as suggested by knobs north of Milankovic crater that grade into a scarp to the east that gradually disappears at ~290°E. The base of the knobs and scarp decrease in elevation from west (–3900 m) to east (–4400 m). North of the center of this boundary are mounds and depressions of Scandia Cavi (down to –5300 m). The mounds and depressions have been attributed to sedimentary volcanism [2], although a glacial origin also has been suggested [9]. These features occur north of Alba Patera and may represent an Early Amazonian phase of HLB-style resurfacing out in the northern plains caused by geothermal and/or climatic heating.

**Discussion.** Hesperian and Amazonian modification of the HLB was dominated by collapse and mass-wasting processes that likely involved ground water and ice. The resulting features have base elevations that correspond with distinct stratigraphic controls and possible geothermal activity.

The most profound stratigraphic control appears to be potential horizons extending hundreds of kilometers from the margins of the Utopia and putative Chryse impact basins as defined by base elevations of collapse features. The depressions decrease in elevation by hundreds of meters to more than a kilometer across radial distances of several hundred kilometers away from the basin margins, which is consistent with circum-basin

stratigraphy formed by impacts into flat-lying strata. The Utopia HLB includes two levels of degradation. The upper one is oldest and coincides with Early Hesperian degradation that forms remnant knobby lowland inliers of Noachian materials common over most of the exposed HLB. The widespread occurrence of this degradation, following the apparent shutdown of widespread valley network dissection, may be related to climate induced processes, such as the formation of a thick cryosphere and perhaps initial development of high pore-water pressures in confined, sub-permafrost aquifers. The younger, lower level is Late Hesperian and coincides with the crater age of the Chryse outflow channels and chaos. The discharge of large volumes of water may have induced climate change [e.g., 10] or resulted in infusion of relatively warm water into lowland rocks.

Origin of the VBF is commonly attributed to a northern plains ocean [e.g., 11]. However, a puzzle is that the VBF embays the outflow channels and has a significantly lower crater density than the outflow materials. It appears that when the VBF formed, it intensely degraded pre-existing craters, including those formed after the outflow channels. One scenario worth entertaining is that the lower boundary plains material, exposed along the Utopia HLB, reflects the margin of a water-rich debris ocean [8] that later underwent melting and periglacial reworking to form the VBF.

Potential geothermal modifications include (1) back-wasting of the HLB, (2) ground-water discharges perhaps accompanied by ground ice melting in regions surrounding the Elysium and Tharsis rises to form collapse structures and outflow channels, and (3) subpolar plains discharges north of Alba Patera. Many of the features are hundreds of kilometers from apparent surface manifestations of volcanism, which indicates that heat may have been transferred through radiating dikes or by hydrothermal circulation of ground water along fracture systems radial to the Tharsis and Elysium rises.

This collective view points to stratigraphic, structural, hydrologic, climatic, and geothermal controls for the modification of the HLB during the Hesperian and Amazonian. Many of the suggested scenarios can be tested and then reworked and refined as needed by further, more detailed mapping of strata, structure, and landforms and more detailed crater counting to achieve more precise historical reconstructions.

**References.** [1] Smith D.E. et al. (1999) Science 284, 1495. [2] Tanaka K.L. et al. (2003) JGR 108, 8043. [3] Skinner J.A. Jr. et al. (2004) this volume. [4] Tanaka K.L. et al. (2003) JGR 108, 8079. [5] Rodriguez J.A.P. et al. (2003) GRL 30, 1304. [6] Rodriguez J.A.P. et al. (2004) LPSC XXXV, #1792. [7] Scott D.H. et al. (1986-87) USGS Maps I-1802A-C. [8] Tanaka K.L. et al. (2001) Geology 27, 427. [9] Fishbaugh K.E. and Head J.W. III (2000) JGR 105, 22,455. [10] Baker V.R. et al. (1991) Nature 352, 589. [11] Parker T.J. et al. (1989) Icarus 82, 111.

## LONG WAVELENGTH TOPOGRAPHY OF THE DICHOTOMY BOUNDARY IN NORTHERN TERRA CIMMERIA: EVIDENCE FOR FLEXURE OF THE SOUTHERN HIGHLANDS

T. R. Watters<sup>1</sup>, P. J. McGovern<sup>2</sup> and R. P. Irwin<sup>1</sup>, <sup>1</sup>Center for Earth and Planetary Studies, National Air and Space Museum, Smithsonian Institution, Washington, D.C. 20560 (twatters@nasm.si.edu); <sup>2</sup>Lunar and Planetary Institute, 3600 Bay Area Blvd., Houston TX 77058.

**Introduction:** In the eastern hemisphere of Mars, the dichotomy boundary is expressed by a significant change in elevation ( $>2$  km) (Fig 1). The dichotomy boundary in this hemisphere is also marked by tectonic features [1]. Fault-controlled fretted valleys or extensional troughs are found in the lowlands [2] and lobate scarp thrust faults are found in the adjacent highlands [3]. Extensional and compressional deformation along the dichotomy boundary appears to have occurred during the late Noachian to early Hesperian [2, 4]. This suggests that tectonism played a role in shaping the present-day dichotomy boundary in the eastern hemisphere. The population of ancient buried impact basins in the northern lowlands suggests that the lowlands crust and the crustal dichotomy formed in the early Noachian [5]. A number of lines of evidence suggest that the slopes of the ancient dichotomy boundary are still preserved [6]. Thus, the present-day boundary in the eastern hemisphere may be the result of late Noachian-early Hesperian tectonic modification of the ancient highlands-lowlands crustal boundary.

**Long Wavelength Topography:** The long wavelength topography along the length of a  $\sim 2100$  km section of the dichotomy boundary in northern Terra Cimmeria has been examined (Fig. 1). This study area includes the  $\sim 200$  km long section of the boundary initially studied by Watters [1]. We find that the dichotomy boundary along much of its length consists of an arching ramp flanked by a broad rise. Topographic profiles across the boundary show that the broad rise is followed by a relatively steep ramp that slopes downward into the lowlands (Fig. 2). Slopes reach a maximum on the ramp and the scarp that marks the dichotomy boundary and are gently sloping away from the boundary on the back rise.

**Flexure Model:** Lithospheric flexure results in long wavelength topography with a distinct deflection profile. The downward deflection of the lithosphere is accompanied by a flanking upwarp or bulge [see 7, 8]. This deflection profile is very similar to profiles of the dichotomy boundary in northern Terra Cimmeria. We model lithospheric flexure of an elastic plate overlying an incompressible fluid subjected to an end load and a bending moment [1]. The model universal flexure profile is valid for any two-dimensional elastic flexure of a semi-infinite lithosphere under an end load [7]. The height of the bulge or rise  $w_b$  and the half-width of the rise  $x_b - x_0$  can be directly measured from topographic profiles. The flexural parameter is

related to the half-width of the rise by  $x_b - x_0 = (\lambda/4)$  [7]. Two well-preserved areas of the dichotomy boundary in northern Terra Cimmeria have been modeled. The topography of the dichotomy boundary in western Terra Cimmeria (Fig. 1) is best fit by  $x_b - x_0 = 120$  km and  $w_b = 600$  m (Fig. 3) [1]. The long wavelength topography of the boundary in eastern Terra Cimmeria is very similar. Here a good fit is obtained by  $x_b - x_0 = 120$  km and  $w_b = 350$  m (Fig. 4). The model fits correspond to an elastic thickness of  $\sim 30$  km, assuming the mean density of the highland of  $2900 \text{ kg}\cdot\text{m}^{-3}$ , a density of the martian mantle of  $3400 \text{ kg}\cdot\text{m}^{-3}$  and a Young's modulus of the lithosphere of  $E = 100 \text{ GPa}$ . Flexure of the highlands may be the result of late Noachian-early Hesperian vertical loading from the emplacement of volcanic material in the northern lowlands [1].

**Broken or Continuous Lithosphere:** The shape of the deflection of the highlands may provide insight into the nature of the transition between the elastic lithosphere of highlands and lowlands (i.e., broken or continuous). This may have important implications for the origin of the crustal dichotomy. The most pronounced difference between the deflection of a continuous or infinite elastic plate and a broken or semi-infinite plate supporting a line load is in the height of the bulge  $w_b$ . For a given load,  $w_b$  for a broken plate is greater than that of a continuous plate (Fig. 5) [see 7, 8]. The slope of the downward deflection or ramp is also less for the continuous plate (Fig. 5). The good fits obtained for the profiles of the dichotomy boundary (Fig. 3, 4) favor a broken or weak contact between the highlands and lowlands lithosphere. A discontinuous lithosphere could have been formed in an early stage of plate tectonics [9], making the dichotomy boundary in the eastern hemisphere analogous to a terrestrial passive margin [1]. However, a continuous highlands-lowlands lithosphere can not be ruled out. Finite element modeling that accounts for the crustal and mantle structure in the area of the dichotomy boundary shows that it may be possible to explain the long wavelength topography and the height of the bulge with a continuous lithosphere [10].

**References:** [1] Watters T.R. (2003a) *Geology*, 31, 271-274. [2] McGill G.E. and Dimitriou A.M. (1990) *J. Geophys. Res.*, 95, 12595-12605. [3] Watters T.R. (2003b) *J. Geophys. Res.*, 108, doi: 10.1029/2002JE001934. [4] Watters T.R. and Robinson M.S. (1999) *J. Geophys. Res.*, 104, 18981-



18990. [5] Frey H.V. et al. (2002) *Geophys. Res. Letts.*, 29, 22-1—22-4. [6] Irwin R.P. and Watters T.R., this volume. [7] Turcotte D.L. and Schubert G. (2002) Cambridge Univ. Press, Cambridge. [8] Watts A.B. (2001) Cambridge Univ. Press, Cambridge. [9] Lenardic A., Nimmo F. and Moresi L. (2004) *J. Geophys. Res.*, 109, doi: 10.1029/2003JE002172. [10] McGovern P.J. and Watters T.R., this volume.

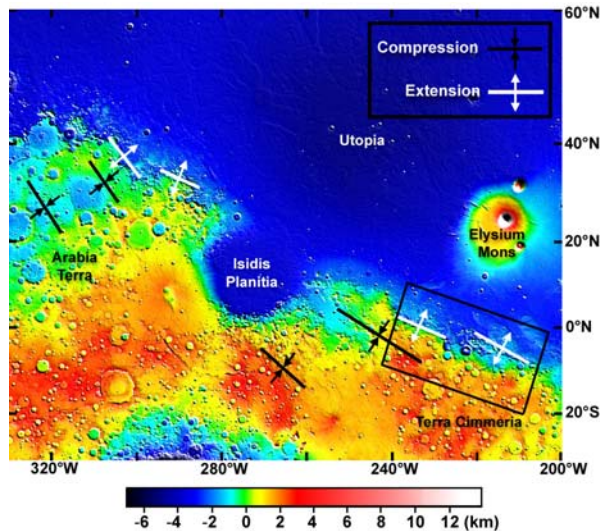


Figure 1. Location of extensional (troughs) and compressional (lobate scarps) tectonic features along dichotomy boundary in the eastern hemisphere overlaid on a color-coded digital elevation model (DEM) combined with a shaded-relief map derived from MOLA  $1/32$  degree per pixel resolution gridded data. Black box shows the approximate location of the study area in northern Terra Cimmeria.

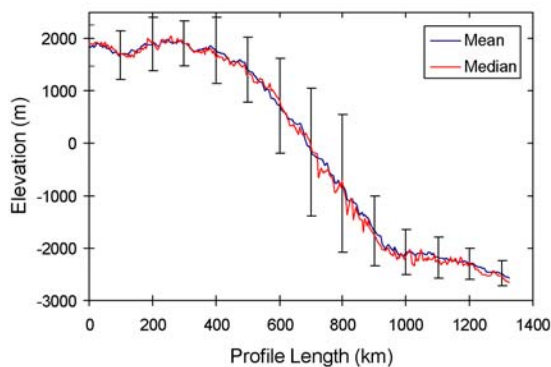


Figure 2. Long wavelength topography of the dichotomy boundary in northern Terra Cimmeria. Topographic profiles are the mean and median of 41 profiles spaced at approximately 50 km intervals covering the area of the boundary shown in Fig. 1. The error bars are 1 standard deviation. Vertical exaggeration is  $\sim 160:1$ .

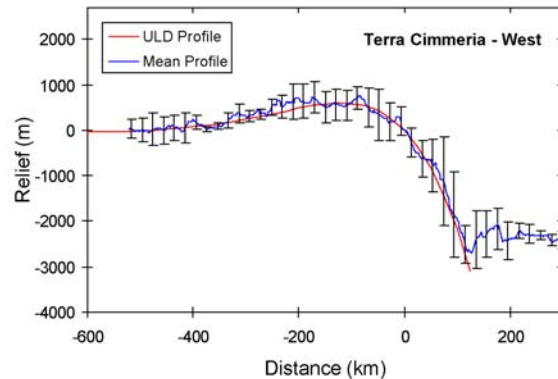


Figure 3. Topographic profile across dichotomy boundary in western Terra Cimmeria compared to a universal lithospheric deflection (ULD) profile. Topographic profile (blue curve) is the mean of the 7 profiles with  $\pm 1$  standard deviation error bars. ULD profile (red curve) was obtained for  $x_b - x_0 = 120$  km and  $w_b = 600$  m. Vertical exaggeration is  $\sim 85:1$ .

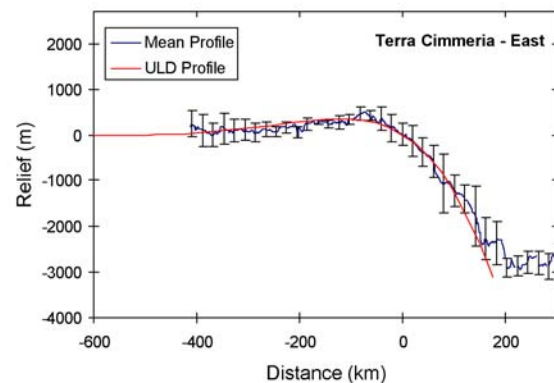


Figure 4. Topographic profile across dichotomy boundary in eastern Terra Cimmeria compared to a ULD profile. Topographic profile (blue curve) is the mean of the 4 profiles with  $\pm 1$  standard deviation error bars. ULD profile (red curve) was obtained for  $x_b - x_0 = 120$  km and  $w_b = 350$  m. Vertical exaggeration is  $\sim 85:1$ .

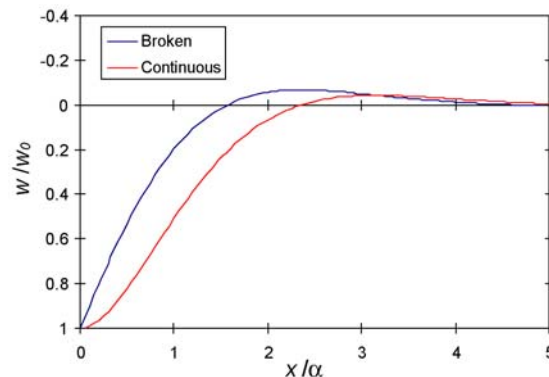


Figure 5. The deflection of a continuous and broken elastic lithosphere under load. The x-axis is the ratio of the deflection  $w$  to the maximum amplitude of the deflection  $w_0$  and  $\alpha$  is the flexural parameter.

**EFFECT OF THE DICHOTOMY ON MANTLE PLUME LOCATIONS** M. J. Wenzel<sup>1</sup>, M. Manga<sup>2</sup>, and A. M. Jellinek<sup>3</sup>, <sup>1</sup>Department of Earth and Planetary Science, University of California, Berkeley, CA 94720; mjwenzel@seismo.berkeley.edu, <sup>2</sup>Department of Earth and Planetary Science, University of California, Berkeley, CA 94720; manga@seismo.berkeley.edu, <sup>3</sup>Department of Physics, University of Toronto, Toronto, Canada; markj@physics.utoronto.ca

**Introduction:** Martian crustal thickness is dichotomous [1]. As the crust is expected to be enriched in heat-producing elements, the temperature at the base of the thicker crust of the southern highlands will be higher than at the base of the northern lowlands. This is analogous to an insulating lid on part of the mantle. It is also possible the martian mantle is compositionally layered [2]. These two effects strongly influence mantle dynamics, including the location and longevity of upwelling plumes [3]. We perform a series of analogue laboratory experiments to examine these effects.

**Experimental methods:** We perform the experiments in a glass-walled, aluminum-floored tank of aspect ratio  $\sim 4$ . The top boundary condition is set to be at a constant temperature by an inset glass tank, filled with well-stirred ice water. To simulate the thicker highland crust, for some experiments 60% of the floor of the inset tank is covered with a 1.27-cm thick acrylic insulating lid. The effective thermal conductivity of the insulated side is  $\sim 40\%$  of that of the side with no insulating lid, equivalent to a crust about twice as thick under the southern highlands [1]. Working fluids are aqueous corn syrup solutions with highly temperature-dependent viscosity, with food dye added to the lower layer. Two opposite sides of the tank are insulated with 5.1-cm-thick polystyrene foam blocks. The two remaining sides are left open so that we can photograph and videotape the experiment. The experiments take one of two forms: (1) bottom heating and top cooling, or (2) secular cooling simulating internal heating. In the experiments with bottom heating, the fluids and the tank are initially at room temperature; the base of the tank is a hollow aluminum heat exchanger, through which hot water is pumped. In contrast, in the experiments with secular cooling the tank base is insulated. The fluids and the tank base are separately warmed and the fluids are then poured into the tank. We then bring the ice bath into contact with the top of the fluid, which results in thermal convection. The system cools over time as heat is lost to the ice bath. We quantify heat transfer during convection with timeseries of temperature and heat flux, measured with thermocouples and heat flux sensors on the tank roof and floor and thermocouple probes within the convecting interior.

**Results:** In the case with no insulating lid, the plume spacing is predicted from linear stability theory to be  $L = C(\nu/Ra)^{1/3}$ , where  $C$  is a constant,  $\nu$  is the ratio of viscosity in the fluid interior to that in the thermal boundary layer, and  $Ra$  is the Rayleigh number (e.g., [4]). The number of plumes ( $n$ ) in the convecting layer is a proxy for the spacing:  $L \sim n^{-1/2}$ . The prediction then is that  $n \sim Ra^{2/3}$ . We count the number of plumes visible in the shadowgraph videos and plot  $n$  as a function of  $Ra$  in Figure 1. The flow is transient by the nature of the secular cooling experiments, and scatter is greatest at earlier times (high  $Ra$ ). Nevertheless, a clear trend is defined, with a slope in  $\log(Ra)$ - $\log(n)$  space of 3, not 1.5 as predicted by theory. One effect of compositional layering is that the topography on the interface stabilizes the locations of upwelling plumes. We argue that the presence of compositional layering slows the reorganization of flow that accompanies a decrease in  $Ra$ . The result is that the number of plumes is higher than would otherwise be predicted at a given point in the planet's evolution.

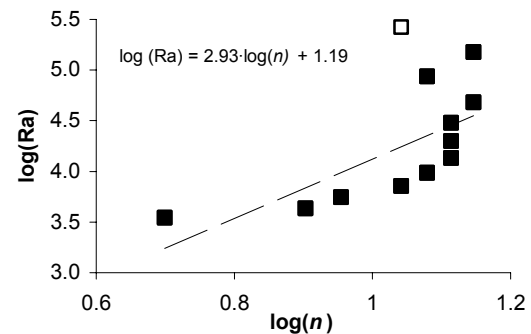


Figure 1:  $\log(Ra)$  v.  $\log(n)$ . Best-fit line excludes first point (open symbol). Slope of  $\sim 3$  is different from predicted slope of 1.5.

In the case with both an insulating lid and layered convection, a strong hot upwelling forms under the lid and persists for the equivalent of many billions of years [3]. If the mantle upwelling leads to melting, volcanic material will be emplaced as crust over the upwelling. The thickening of the crust will reinforce the difference in insulation that localizes the upwell-



ing—that is, there is a positive feedback between crustal thickness and mantle upwelling.

**References:** [1] Zuber M. T. et al. (2000) *Science*, 287, 1788-1793. [2] Elkins-Tanton, L. T. et al. (2003) *Meteoritics and Planet Sci.*, 38, 1753-1772. [3] Wenzel, M. J. et al. (2004) *GRL*, 31, L04702. [4] Jellinek, A. M., and Manga, M., *Rev. Geophys.*, in press.

**On The Dynamic Origin Of The Crustal Dichotomy and Its Implications For Early Mars Evolution.** Shijie Zhong, James H. Roberts and Allen McNamara, Department of Physics, University of Colorado, Boulder, Colorado 80309, USA (szhong@anquetil.colorado.edu).

**Introduction:** The crustal dichotomy and Tharsis Rise are the most important large-scale tectonic features on the Martian surface [1]. An understanding of their formation has important implications for understanding thermal evolution of Mars and the Martian gravity anomalies, tectonics, volcanism, and volatiles losing history [2,3]. Both endogenic and exogenic processes were proposed for the formation of the crustal dichotomy. In this study, we focus on endogenic processes. Two different endogenic processes were proposed: crustal erosion derived from degree-1 mantle convection [4] and plate tectonics [5], both proposed before the MGS missions.

With the MGS high resolution data, there are a number of studies on the nature of Martian crust, crustal dichotomy and Tharsis rise that should be considered in any attempts to unravel the formation of crustal dichotomy and the evolution of early Mars. 1) The discovery of abundant buried ancient impact craters in the northern plains indicates that the crust of the northern hemisphere is of the middle Noachian or as old as that of the southern hemisphere, if not older [6]. 2) The topography and gravity anomalies suggest a pole-to-pole gradual and smooth variation of crustal thickness [7]. 3) The topography and gravity anomalies suggest that Martian crust is on average >50 km thick and is thicker than the elastic plate (or the layer that is capable of supporting long-term geological loads) [7,8]. Not only the surface but also the bulk of the crust may have been produced quite early on (in the first 0.5 Ga), according to the thermal evolution modeling [9]. 4) Significant tectonic deformation occurred along the crustal dichotomy in late Noachian and early Hesperian [10]. 5) The surface tectonics suggest that the bulk of the Tharsis rise was formed by the late Noachian [11,4], similar to the formation time of crustal dichotomy. Modeling the Tharsis topography and gravity indicates that the Tharsis rise is mostly supported by surface loads on elastic plate with little or no dynamic contribution from a plume [12].

Among the two proposed endogenic processes (i.e., crustal erosion and plate tectonics) for crustal dichotomy formation, a necessary process is the degree-1 mantle convection in which hot upwellings preferentially occurs in one hemisphere while cold downwellings are in other hemisphere. Such a degree-1 mantle convection is also required for a plate tectonic process to explain the formation of crustal dichotomy, although this was never explicitly stated before (why does it occur only in the northern hemisphere?). However, the physical conditions under which mantle convection forms degree-1 structure are not well understood [13,14,15]. Furthermore, even if degree-1 mantle convection is achieved, it is unclear how degree-1 mantle convection could lead to crustal dichotomy and how crustal dichotomy

could be preserved through the Martian geological history [15]. In addition to crustal dichotomy, the formation of the Tharsis rise also needs a largely degree-1 mantle convection or a one-plume convection that operated during late Noachian period, following the formation of crustal dichotomy [12]. Although the Tharsis rise is centered at the dichotomy boundary not below either of the hemispheres, the similarity in mantle dynamics is intriguing.

There are two goals of this study: 1) to critically review all the published mantle dynamic models for degree-1 mantle convection and to explore new and more realistic mantle parameter space for degree-1 mantle convection; 2) to synthesize surface observations and mantle dynamic models for a coherent picture for the early evolution of Mars.

**Degree-1 mantle convection:** Two different mechanisms have been proposed for degree-1 or one-plume mantle convection for Mars: 1) one-plume convection derived from exothermic or endothermic phase changes that was initially proposed for a dynamic support for the Tharsis rise [13,14], and 2) degree-1 convection caused by layered viscosity proposed to explain the formation of crustal dichotomy [15].

The effects of exothermic phase change on one-plume convection [14] were questioned in [16] that showed that the actual effects seen in [14] are caused by the moderately high viscosity lithosphere. There are two potential problems with the endothermic phase change models: 1) existence of such an endothermic phase change given the recent estimate of core size [17], and 2) the published models with phase changes were done with only moderate depth-dependent viscosity and no temperature-dependence. Our calculations with the endothermic phase change, while reproducing one-plume structure with no temperature-dependent viscosity, fail to produce one-plume structure with more realistic temperature-dependent viscosity [18]. The models with layered viscosity structure that produced degree-1 convection used a temperature- and pressure-dependent viscosity, but the models were done in 2-D axisymmetric models [15]. It is important to examine the effects of 3-D geometry on the flow.

We have recently explored the layered viscosity models in 3D spherical geometry with temperature- and pressure-dependent viscosity and pressure-dependent thermal expansion coefficient and thermal diffusivity [18]. Our calculations showed that degree-1 convection remains with 3D layered viscosity models. However, it appears that a smoothly varying viscosity with depth is not as effective as a step function like increase of viscosity in producing degree-1 convection. This suggests that either non-Newtonian viscosity or viscosity change caused by the olivine-spinel phase change may be essential.

Two end-member models for Martian mantle convection are the stagnant-lid convection and plate-tectonic style convection [5,19]. However, while the evidence for early plate tectonic process on Mars is still elusive, the application of stagnant-lid convection may also be problematic. It is well known that stagnant-lid convection in its original form often leads to small-wavelength structures [20], which is in sharp contrast with crustal dichotomy and Tharsis rise that are both of very long wavelength. We propose that for early Mars the crust may play an active role in controlling heat transfer and mantle structure, if the crust was indeed  $>50$  km thick. The key components of our proposal are that the lower crust for early Mars may be sufficiently weak to serve effectively as free-slip boundary condition for the mantle and that the thickened crust increases the mantle lithospheric temperature so that the mantle lithosphere may be able to deform. The net effect for mantle convection is that mantle lithosphere may be mobile with only moderate viscosity contrast with respect to the underlying asthenosphere. In this scenario, the crust may be the limiting factor for heat transfer. If the lower crust is sufficiently weak that convection can take place there (i.e., crust convection), then crust may transfer heat efficiently out of the mantle. If crust convection cannot happen, then heat has to transfer conductively through the crust.

We have computed 3D spherical models with free-slip top boundary and moderate temperature-dependent viscosity that approximate the effects of the crust. We found that degree-1 convection may be produced within certain model parameter space. In particular, when large internal heating is included, the lithospheric viscosity becomes sufficiently large compared with the interior viscosity and degree-1 convection is achieved.

**Degree-1 mantle convection and crustal dichotomy and Tharsis rise:** Two possible scenarios were proposed in [15] to link degree-1 mantle convection and crustal dichotomy. 1) The southern hemisphere with thickened crust was formed above the upwellings of degree-1 convection due to melting and the significant fraction of the crust was created during the formation of the dichotomy. 2) The southern hemisphere was formed above the downwellings of degree-1 convection due to shear coupling between the mantle and crust that produces crustal convergence towards the southern hemisphere, and the bulk of the crust may be produced uniformly before degree-1 mantle convection occurs. The first scenario may imply that the southern hemisphere with newly produced crust is younger than the northern hemisphere. That this scenario permits an old northern hemisphere is consistent with the old crust age as suggested in [6]. The second scenario implies that the northern hemisphere is younger (but not much younger) than the southern hemisphere, as the crustal thinning there would lead to some amount of volcanisms in the northern hemisphere. Therefore, it seems that the relative ages of the two hemispheres are important in distinguishing these two scenarios.

With either scenario, as long as the degree-1 mantle convection is active for sufficiently long time, to maintain crustal dichotomy does not seem to be a problem. This is because mantle convection can have significant effects on crustal relaxation.

Finally, given the relatively short time span between the formation of crustal dichotomy and Tharsis rise and the fact that they both should be related to degree-1 mantle convection, it is interesting to consider how degree-1 mantle convection may shift its centers. We will speculate the role of melting in degree-1 mantle convection.

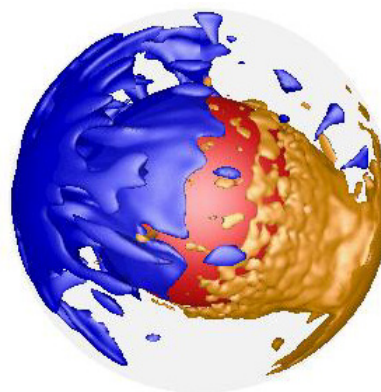


Figure 1. Degree-1 convection from models with moderate temperature-dependent viscosity [21].

**References:** [1] Smith et al. (1999) *Science* 286, 94-97. [2] Solomon & Head (1990) *JGR* 95 11073-11083. [3] Phillips et al. (2001) *Science* 291 2587-2591. [4] McGill & Dimitriou (1990) *JGR* 95 12595-12605. [5] Sleep (1994) *JGR* 99 5639-5655. [6] Frey et al. (2002) *GRL* 29 1387. [7] Zuber et al. (2000) *Science* 287 1788-1793. [8] McGovern et al., (2002) *JGR* 107. [9] Hauck & Phillips (2002) *JGR* 107 5052. [10] Watters (2003) *Geology* 31 271-274. [11] Anderson et al. (2001) *JGR* 106 20563-20585. [12] Zhong & Roberts (2003) *EPSL* 214 1-9. [13] Harder & Christensen (1996) *Nature* 380 507-509. [14] Berner et al. (1998) *GRL* 25 229-232. [15] Zhong & Zuber (2001) *EPSL* 189 75-84. [16] Harder (2000) *GRL* 27 304-307. [17] Yoder et al (2003) 300 299-303. [18] Roberts & Zhong, this volume. [19] Lenardic et al. (2004) *JGR* 109 E02003. [20] Ratcliff et al. (1997) *Physics D*. [21] McNamara & Zhong (2004) in preparation.